JOURNAL
OF
GEOMAGNETISM
AND
GEOELECTRICITY

VOL. XII NO. 1

SOCIETY
OF
TERRESTRIAL MAGNETISM AND ELECTRICITY
OF
JAPAN

1 9 6 0
KYOTO

JOURNAL OF GEOMAGNETISM AND GEOELECTRICITY

The fields of interest of this quarterly Journal are as follows:

Terrestrial Magnetism	Aurora and Night Airglow
Atmospheric Electricity	The Ozone Layer
The Ionosphere	Physical States of the Upper Atmosphere
Radio Wave Propagation	Solar Phenomena relating to the Above Subjects
Cosmic Rays	Electricity within the Earth

The text should be written in English, German or French. The price is set as 1 dollar per number.

The Editors

Diurnal Variation in Atmospheric Electricity

By Toshio OGAWA

Geophysical Institute, Kyoto University
(Read May 16, 1960; Received June 25, 1960)

Abstract

In order to eliminate short-period fluctuations due to local effects, daily courses of potential gradient, conductivity and air-earth current were smoothed out by taking hourly overlapping means of 5 hours and the interrelationship between each element was examined on every day. In urban district, the production of man-made nuclei begins following human activity in the early morning before sunrise and they accumulate in the lowest stable layer of the exchange layer. In the daytime, when the wind rises, the nuclei are transported into the upper layers in the exchange layer by vertical turbulent mixing due to forced convection, and there diffused out horizontally. The eliminated short-period fluctuations are on the average 27% of the concerned elements. Examining diurnal variations of the fluctuations, there is neither evidence that they are caused by local generators other than the thunderstorm generator nor evidence that they are directly connected to strength of turbulence of the air.

1. Introduction

The factor which is chiefly responsible for the diurnal variation of potential gradient on land stations is nucleus concentration on the surface of the earth. The nuleus concentration depends not only on the production of nuclei but also on the dissipation of them. On oceans and polar regions, where there is no production of nuclei and hence no dissipation, the potential gradient shows the world-wide variation with one maximum at about 1900 GMT. On land areas, the characteristic and well-known double-periodic curves of diurnal variation of the potential gradient are obtained. The effect of the production of nuclei is represented by so-called Brown's 24-hour wave with a maximum in the afternoon, while the effect of the dissipation of nuclei is represented by the Brown's depression in the afternoon (Brown, 1935). Israël (1953) attributes the former to the variation of columnar resistance and the latter to a change of local conductivity close to the surface of the earth.

Up to date, in general, discussions of the diurnal variation in atmospheric electricity have been made for the statistical results of each element. As the atmospheric electrical situation, however, varies day after day as well as from place to place even in fair weather, it is desirable to see the above relation on each day. Israël (1955) showed the day-to-day variations of potential gradient, air-earth current and conductivity from July 1 to September 10, 1953 at Buchau, but it is difficult to draw any definite relation between each element.

Mühleisen (1956) pointed out that positive space charges artificially produced on land areas are also causes of the deviations of the diurnal courses of potential gradient and air-earth current from the world-wide course on the oceans. Mühleisen (1958) also pointed out that there are three generators in atmospheric electricity: (1) the thunderstorm and precipitation-generator, (2) the evaporating-generator and (3) the man-made space-charge generator. The evaporating-generator causes the sunrise effect as well as many other local phenomena and the man-made space-charge generator causes the intense fluctuation of the potential gradient. These will be also the reason why the mechanism of the diurnal variation in atmospheric electricity is obscure in daily recording.

In this paper, through exact measurements, the changes of conductivity corresponding to the depression of potential gradient are searched. Eliminating the fluctuations due to local effects in daily records from day to day, diurnal courses in atmospheric electricity are extracted and discussed. Eliminated fluctuations are also examined to look for the origin of themselves.

2. Circumstance of Measurements

The potential gradient, the conductivity and the wind velocity were simultaneously recorded on a recording paper, the running speed of which is 25 mm per hour. Continuous recording of the potential gradient was also made on another recording paper with higher resolving power of time of 60 mm per hour. A generating voltmeter-type fieldmeter was used for the potential gradient and two Gerdien-type conductivity-meters with vibrating-reed electrometers of response time within 2 seconds were used for the polar conductivities. These apparatus were set atop the building of the Geophysical Institute of Kyoto University about 15 m high to avoid direct effects of pollution produced at the ground. The Institute is located in the north-east district of Kyoto city, which has the population of about one million and no big industrial area.

3. Elimination of short-period fluctuations

The statistical results from a great deal of data are generally used to see the atmospheric electric daily variations. At any instant, however, measured values in atmospheric electricity are subjected to fluctuations and hourly values of the elements deviate much from daily courses of variations. Here, in order to eliminate such short-period variations, measured values are smoothed out by taking overlapping means.

In the first place, the period to take overlapping means must be decided. Fig. 1 shows an example of the fluctuations in the potential gradient, the conductivity and the air-earth current in the calm night of March 22–23, 1960. Because of the inverse relation between the potential gradient and the conductivity, the air-earth current given by the product of them is expected to be less subject to fluctuations. The values of the air-earth current calculated every 1.5 min are, however, contrary to this expectation as shown in Fig. 1. Then firstly are obtained the overlapping mean values of 30 min which covers the maximum relaxation time during the concerned period. Next, the period for taking overlapping means are extended until the fluctuations

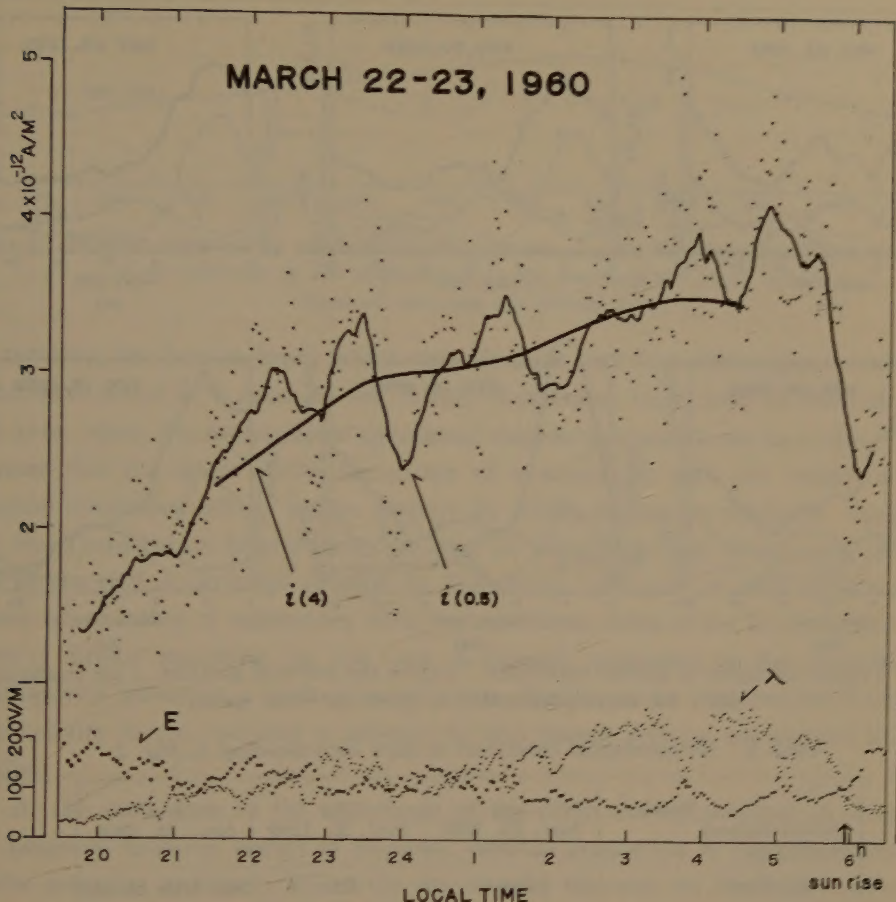

Fig. 1. An example of short-period fluctuations in atmospheric electric elements on March 22–23, 1959. E gives the potential gradient and λ the conductivity. i gives the air-earth current calculated from E and λ. i (0.5) and i (4) show the overlapping mean curves of 30 min and 4 hours in the air-earth current.

vanish. When 4 or 5 hours is taken for the period, it is found that the fluctuations are almost eliminated and the diurnal courses of elements are characterized. In practice, the period was taken as 5 hours when hourly values were used. Thus the elimination of short-period fluctuations was carried out every day.

4. Diurnal Variation

Some of the results for the days without precipitation are given in Fig. 2, corresponding to which meteorological conditions are listed in Table 1. In the diurnal courses there are four types of variation paying attention to the effect of the wind. (1) The windy time is restricted in the daytime ($a_{1,2}$). (2) The windy time is ranged from the daytime to midnight ($b_{1,2}$). (3) There is no wind ($c_{1,2}$). (4) There is a continuous wind.

The following mechanism of the diurnal variation in the atmospheric electric field is suggested in daily smoothed diurnal curves of variation, several examples of which

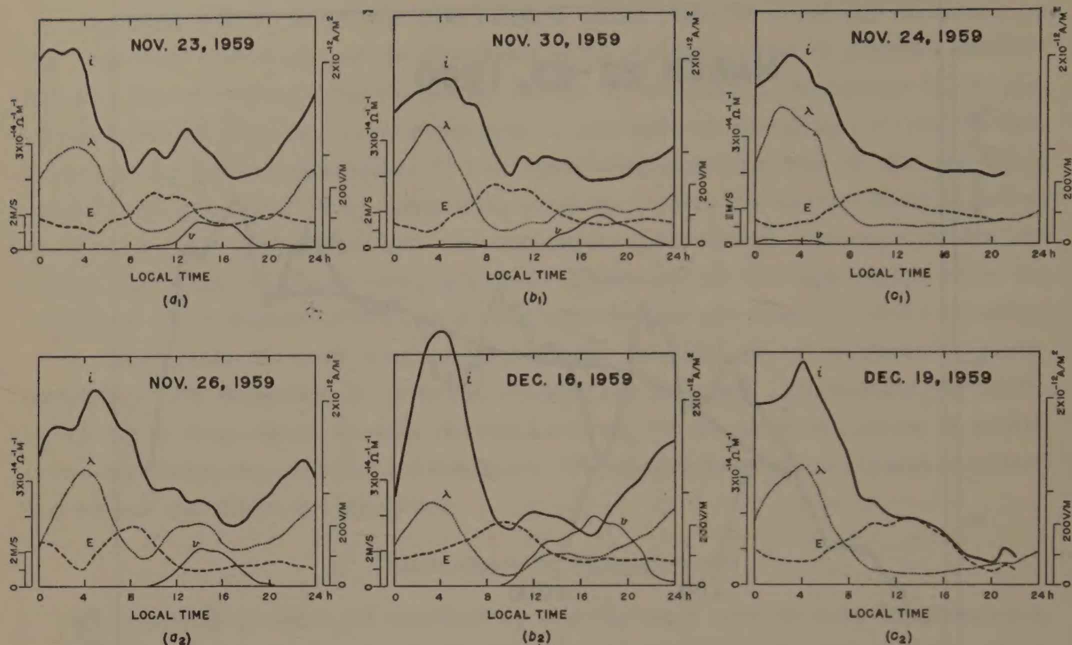

Fig. 2. Typical examples of diurnal variations. E gives the potential gradient, λ the conductivity and i the air-earth current. v gives the wind speed.

Table 1. Meteorological conditions in days corresponding to Fig. 2

Meteorological conditions \ Dates	(a_1) Nov. 23, 1959	(b_1) Nov. 30, 1959	(c_1) Nov. 24, 1959
Weather	fine	fine	fine, later cloudy
Cloudiness average, 0–10	4.0	0.0	6.8
Wind speed average (m/s)	1.1	0.9	0.9
Sunlit time (hour)	8.7	8.5	6.4
Meteorological conditions \ Dates	**(a_2) Nov. 26, 1959**	**(b_2) Dec. 16, 1959**	**(c_2) Dec. 19, 1959**
Weather	fine, occasionally cloudy	fine, occasionally cloudy	fine, later cloudy
Cloudiness average, 0–10	6.5	8.0	8.3
Wind speed average (m/s)	1.8	1.9	0.8
Sunlit time (hour)	5.5	4.1	1.8

are shown in Fig. 2. In the early morning before sunrise, the conductivity begins to decrease. According to Chalmers (1957), " the fine-weather conductivity at many places shows a maximum in the early morning hours, with a fall soon after sunrise." However, it must be noticed that in the present measurements the occurrence time of a fall of conductivity in the morning is always earlier than the time of sunrise. In Fig. 3 are shown the times of beginning of a fall of conductivity together with the times

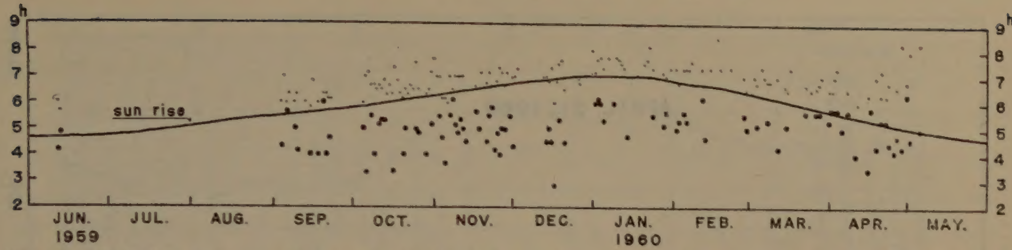

Fig. 3. Relation between the conductivity and sunrise. Large dots show the times of beginning of an decrease in the conductivity in the morning and small dots the times of reaching the bottom level.

of reaching the bottom level, which were directly read from the original records. The occurrence times of a decrease are mainly distributed from 0400 to 0600 throughout the year, when the atmospheric dynamical state is most stable during a day. This will suggest that the origin of the decreasing of conductivity does not relate to meteorological conditions but to human activity by which nuclei are produced. Inquiring of the Gas Company in Kyoto about the time of a morning rise of the used amount of gas in the city, it occurred at 0400 in November, 1959 and at 0500 in March, 1960, which are roughly in agreement with the occurrence times of the decreasing of conductivity. Either gas-using in the city is directly connected to the morning fall of conductivity leaves to a further investigation, but it can be said that the decreasing of conductivity in the morning is affected by the human activity represented by the use of gas.

At the same time as the occurrence of the early moring decrease of conductivity, the potential gradient begins to increase; nucleus production is also the origin of rise of the potential gradient. When the sun rises in the way of these processes i.e. the decreasing of conductivity and the increasing of potential gradient, no effect of the sunrise on the diurnal courses can be seen.

The first minimum of conductivity and the first maximum of potential gradient occur at about 0900, from which onwards the decreasing of air-earth current slacks up. This effect is also clear in the columnar resistance which slows down the increasing rate of itself. In these processes of conductivity, potential gradient, air-earth current and columnar resistance, occurrence of the wind has a fundamental importance; these processes follow the commencement of the wind which causes the second maximum of conductivity and the depression of potential gradient in the afternoon. When there is no wind, the conductivity has no second maximum and the potential gradient does not show the depression. This is clear in (c_1) and (c_2) of Fig. 2.

Thus it appears to be legitimate to assume that the factor which is chiefly responsible for the transfer of nuclei in the vertical is forced convection, i.e. the removal of nuclei from near the ground causing the depression of the potential gradient is due to turbulence in moderate or high wind. On the other hand, free convection which begins soon after sunrise does not seem to have direct effect on the electric field.

The variation of conductivity in the daytime depends sensitively on the wind speed as shown in Fig. 4. When the wind is getting up the conductivity increases from the

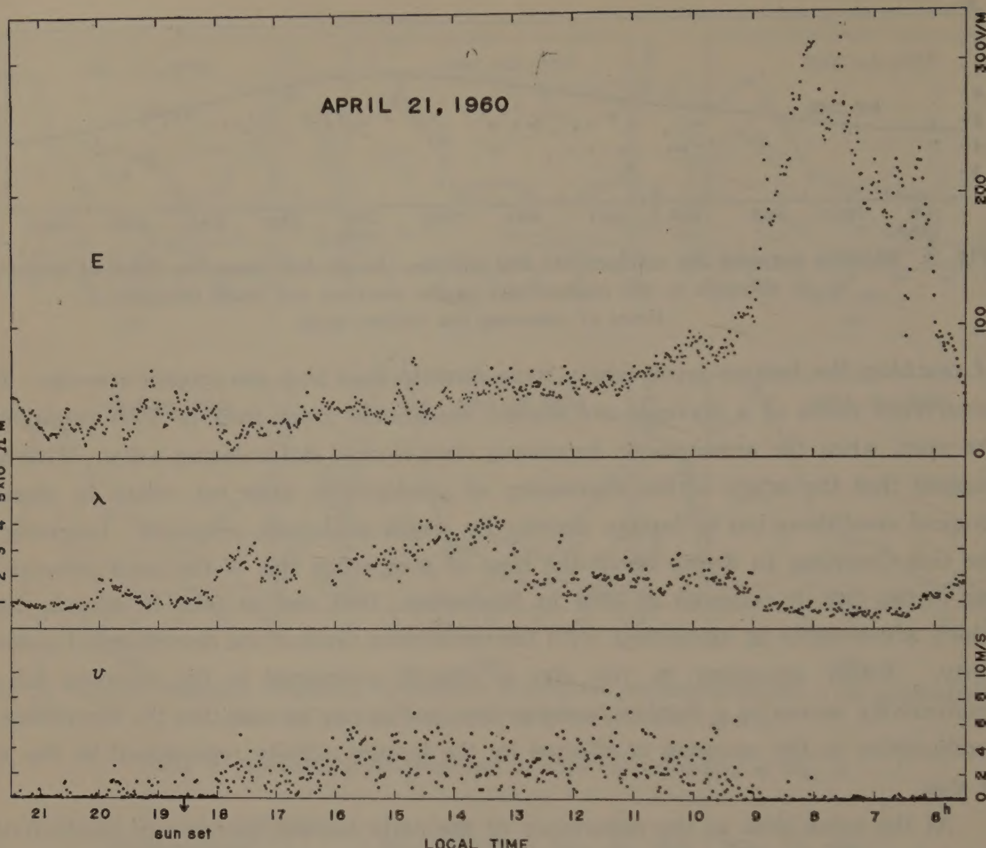

Fig. 4. Typical example of dependence of the conductivity (λ) on the wind speed (v). E gives the concurrent potential gradient on April 21, 1960.

bottom level, and when the wind is going down the conductivity returns the bottom. The simultaneity of both phenomena is higher in the latter case than in the former one. This fact suggests that the accumulation of nuclei which make the conductivity decrease and then the potential gradient increase, undergoes in the lowest restricted layer of the exchange layer. This effect is clearer in a day of clear sky. It should be noted that it is one of the most important problems to know the depth of this lowest restricted layer in rlation to the urban sanitaion.

If above mentioned idea is acceptable, occurrence of the maxima of potential gradient will be controlled by the time of occurrence of the wind. Three typical examples of the potential gradient are shown in Fig. 5 which contains continuous recording on April 6, 21 and 26, 1960. The first maxima of potential gradient appear at about 0830 on April 6, 0800 on April 21 and 0730 on April 26. There are evidences in another recording that the wind began to blow little after the maxima. It is noticed that the period of short-period variations changes towards smaller from before to after the maxima ; before the maxima, the variations with periods of 10–20 min predominate, while the variations with periods of 1–5 min become predominant after the maxima.

In the windy time, the mixing is so thorough that the nucleus distribution near the ground tends to become uniform with height. In this condition, there is no large-

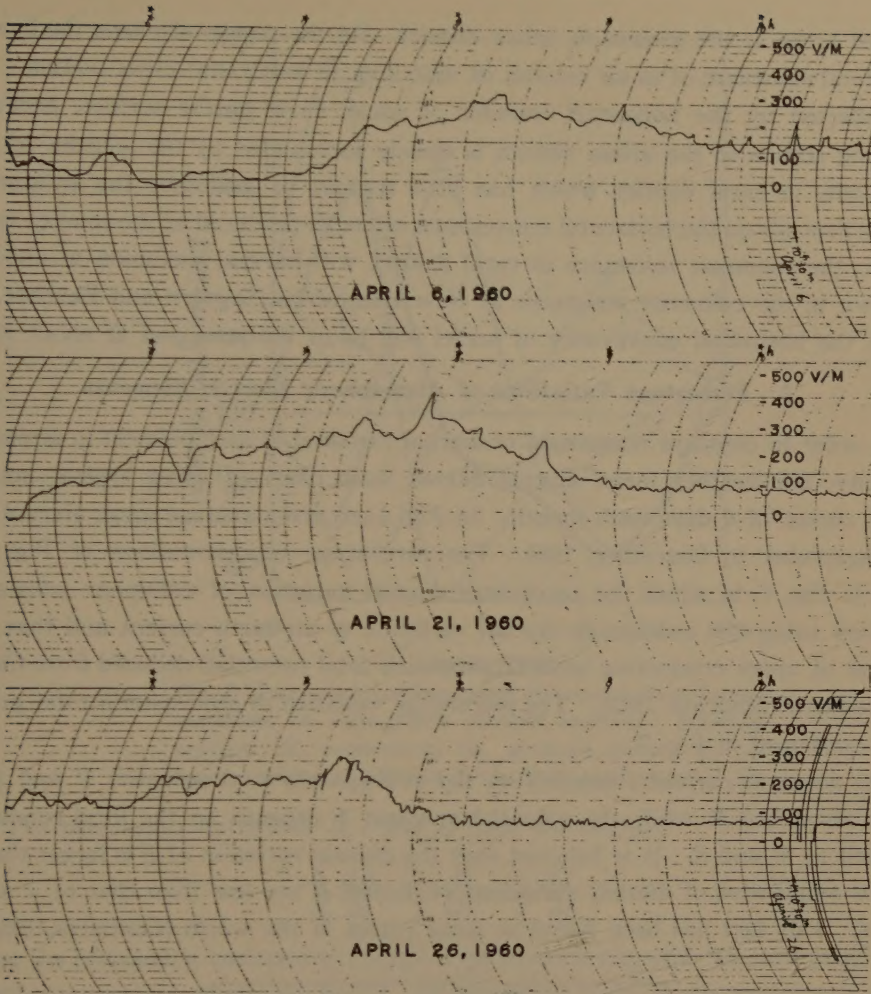

Fig. 5. Typical examples showing the first maxima of potential gradient in 3 individual days in April, 1960.

scale nucleus-concentration in the air but only small-scale one affects on the atmospheric electric field. It results in predominance of short-period variations due to contribution of small-scale nucleus-concentrations (refer to Ogawa, 1960a, as to the concept of the "scale" in the atmospheric electric field).

The second maximum of potential gradient is similarly circumstanced to the first maximum brought with a reverse process of change; the occurrence time of second maximum is controlled by the subsidence time of the wind in the evening. When the wind does not fall at the evening, the conductivity turns to the night increase without second minimum, and thus there is no second maximum of potential gradient. The examples of this case are shown in (b_1) and (b_2) of Fig. 2.

In conclusion, the stagnations of air-earth current and columnar resistance during the time from about 0900 to 1700 should be considered. When accumulated nuclei in the lowest restricted layer are transported into the upper layers by turbulent vertical mixing they are diffused out horizontally, because the sources of pollution have some

localized areas at the ground in urban district. As the results slackens the increasing of the total resistance of an air column of unit area in horizontal cross section. It will be unaffected by the horizontal transfer of nuclei close to the surface, because the observing station in the urban district is closely surrounded by the sources of nuclei. Meanwhile, in rural district which has little sources of pollution the columnar resistance depends on the horizontal conveyance of nuclei produced at the sources in urban district; the columnar resistance in rural district will have a maximum at about 1500 as shown in the columnar resistance at New Hampshire (Sagalyn and Faucher, 1956), that is, the horizontal conveyance of nuclei will be of the strongest at about 1500.

5. Percentage Variations of Atmospheric Electric Elements

In order to compare magnitude of diurnal variation of each element in atmospheric electricity, fair-weather mean diurnal curves were obtained using typical smoothed diurnal curves of 6 days each month. In Fig. 6 are given average mean diurnal curves from September to December, 1959. The percentage representations of Fig. 6 are shown in Fig. 7, in which the percentage diurnal variation of columnar resistance is calculated using the percentage diurnal variation of air-earth current and that of the potential of upper conducting layer (atmospheric total potential) deduced from *Carnegie* measurements (Mauchly, 1923). The percentage variation of atmospheric total potential is also contained in Fig. 7.

The air-earth current i depends on the atmospheric total potential V and the columnar resistance R, while the potential gradient E depends on the local conductivity λ as well as V and R. It is believed that the diurnal variation of E is larger than that of i, for amplitudes of diurnal variations of V and R are less than that of λ in land stations. This fact has been found at some places in the world (Chalmers, 1957).

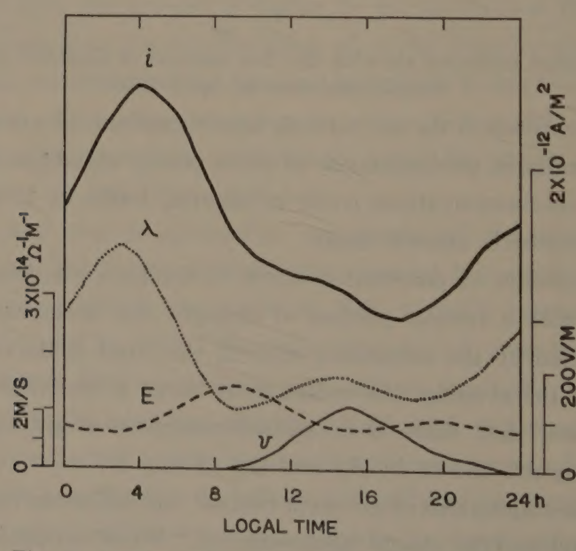

Fig. 6 Average mean diurnal variations of potential gradient (E), conductivity (λ) and air-earth current (i). v gives the wind speed.

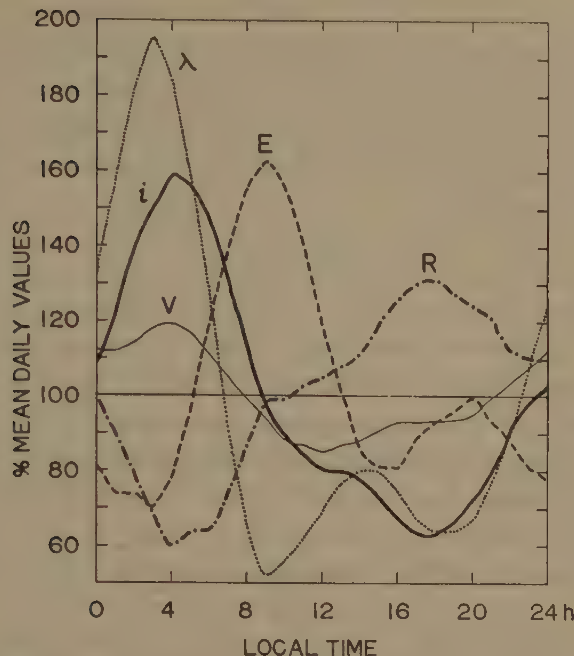

Fig. 7 Percentage representation of average mean diurnal variations of atmospheric electric elements: potential gradient (E), conductivity (λ), air-earth current (i), columnar resistance (R) and atmospheric total potential (V).

The percentage variations of i and E have the relation:

$$\frac{1}{E}\frac{dE}{dt}=\frac{1}{i}\frac{di}{dt}-\frac{1}{\lambda}\frac{d\lambda}{dt}.$$

When the percentage variation of i is out of phase with that of λ, the percentage variation of E is larger than those of i and λ. On the other hand, if the percentage variations of i and λ are of in-phase, there is a case in which the percentage variation of E is less than that of i. As types of the diurnal variation of i have different amplitudes and different initial-phases in different longitudes of the world (Ogawa, 1960b), it cannot always be said that the percentage variation of E is larger than that of i. As shown in Fig. 7 the variations of i and λ are nearly of in-phase and the percentage variation of i is somewhat larger than that of E. In Table 2 are given the values of double-amplitudes of λ, i, E and R; they represent the values at the urban district of the meridian 135°E. The percentage variation of R is a half of that of λ. The value with

Table 2. Amplitude of diurnal variation in atmospheric electric elements: conductivity (λ), air-earth current (i), potential gradient (E) columnar resistance (R) and atmospheric total potential (V)

	λ	i	E	R	V
Double-amplitude of diurnal variation in percentage	143 %	96 %	93 %	71% (35%)	34%

brackets in R represents the value at the rural district referring to the measurements by Sagalyn and Faucher (1956). In Table 2 is also contained the value of V deduced from the measurements on the oceans by the *Carnegie*, which is about half of the value of R in the urban district and is equal to that in the rural district. Thus the variation of V cannot be neglected as compared with R in any case in the atmospheric electric current system over continents.

6. Fluctuations

What is responsible for the origin of fluctuations eliminated in order to see the diurnal course in atmospheric electricity? Here, fluctuations are referred to the differences between the hourly values and the overlapping mean values at any time.

In the first place, the values of root mean square (RMS) of fluctuations σ_i, σ_E and σ_λ during a day are compared with the daily mean values of concerned elements. In Fig. 8 are shown the results obtained on 24 days, diurnal curves of which were used to give the average mean diurnal curves as shown in Fig. 6. In the air-earth current and the potential gradient, the RMS values are nearly proportional to the daily mean

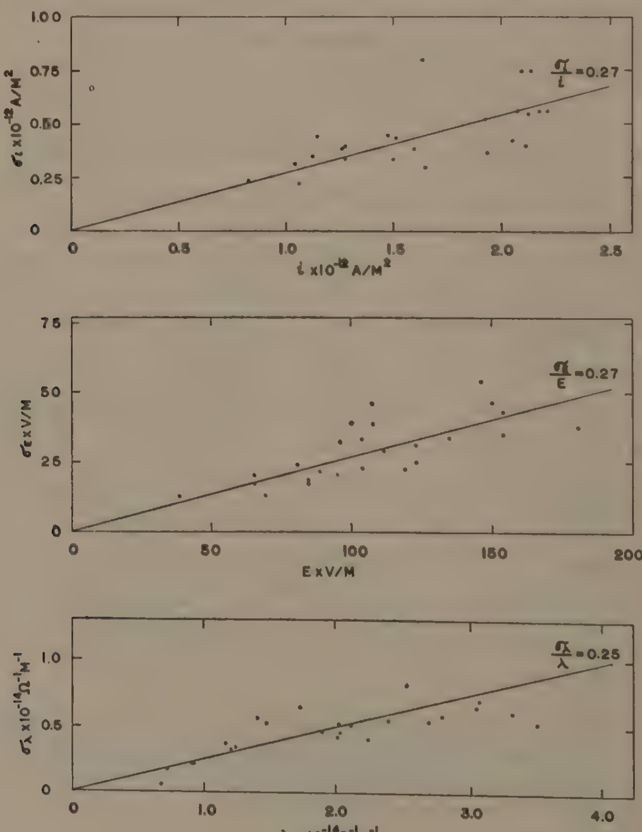

Fig. 8. Diurnal mean values for RMS of fluctuations of potential gradient (E), conductivity (λ) and air-earth current (i) in relation to diurnal mean values of concerned factor itself.

values of elements and are on the average 27% of them. In the conductivity, however, the ratio of the RMS to the daily mean values does not converge to any definite value but tends to saturate in higher daily mean values.

In order to examine the facts mentioned above, the daily variations of RMS are obtained every month. In Fig. 9 are shown the average daily variations of $\frac{\sigma_i}{i}$, $\frac{\sigma_E}{E}$ and $\frac{\sigma_\lambda}{\lambda}$ during the period from September to December, 1959. $\frac{\sigma_i}{i}$ and $\frac{\sigma_E}{E}$ show little variation around the mean value of 0,27, while, $\frac{\sigma_\lambda}{\lambda}$ shows a distinct variation with the mean value of 0.25.

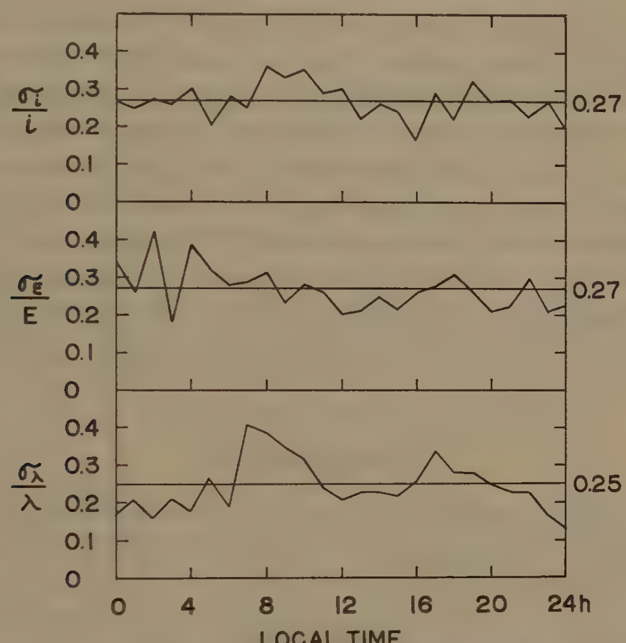

Fig. 9. Average mean daily cycle of RMS of fluctuations of potential gradient (E), conductivity (λ) and air-earth current (i).

In Fig. 9 there is neither evidence that the fluctuations are caused by local generators pointed out by Mühleisen nor evidence that they are directly related to strength of turbulence of the air. If these generators or turbulence of the air are the origins of the present fluctuations, $\frac{\sigma_i}{i}$, $\frac{\sigma_E}{E}$ or $\frac{\sigma_\lambda}{\lambda}$ must be larger in the daytime than in the night-time.

Lastly the diurnal variation of $\frac{\sigma_\lambda}{\lambda}$ should be considered but any conclusive explanation has not been led. The diurnal variation of it is reverse to that of conductivity itself and is parallel to that of potential gradient; is it impossible that the potential gradient has some effects on the fluctuations of conductivity?

7. Concluding Remarks

The effect of the wind on the potential gradient has been found by several

authors. Brown (1936) found that the local effect consisting of a 24-hour wave together with a depression is much reduced when there is a continuous wind which was considered to prevent convection of space charge. In the present paper, however, the wind is conductive to convection and promote the vertical transport of nuclei by turbulent mixing. Sapsford (1936) pointed out that the wind direction has a first importance in the maxima of potential gradient. In the present study such effect cannot be found out. Yokouti (1938) compared the mean diurnal variation curve of potential gradient with that of the wind and suggested that there is a certain correlation between both variations.

Israël (1958) defined the agitation whose amplitude gives the breadth of fluctuation within one hour and whose frequency gives the number of reversal points within one hour. He showed the typical diurnal variation of agitation parameters; the amplitude and the frequency increase from night-time to daytime, and from the evening onwards this process seems to reverse. He has concluded that the mechanism which gives rise to the agitation should be connected with the atmospheric turbulence. On the contrary, the fluctuations in the present paper do not show the same property. Moreover, there is even a tendency that relative magnitude of the fluctuations is smaller in the turbulent condition of the air. This difference between the agitation and the present fluctuation is originated from the difference of the object of study; the agitation is related to the phenomena within one hour, while the fluctuations to the phenomena within five hours.

Aknowledgement

The author wishes to express his sincere thanks to Prof. Y. Tamura for his kind guidance and encouragement throughout the work. He also wishes to thank Mr. S. Saga for his valuable discussions.

References

Brown J.G. (1935) Terr. Megn. Atmos. Elect. **40**, 413.
Brown J.G. (1936) Terr. Magn. Atmos. Elect. **41**, 279.
Brown J.G. (1937) Terr. Magn. Atmos. Elect. **42**, 163.
Chalmers J.A. (1957) *Atmospheric Electricity*. Pergamon Press, London. 133, 142.
Israël H. (1953) *Thunderstorm Electricity*. Univ. Chicago Press, Chicago. 4.
Israël H. (1955) Proc. Conf. Atmos. Elect., Geophys. Recer. Pap. **42**, (AFCRC) 11.
Israël H. (1958) *Recent Advances in Atmospheric Electricity*. Pergamon Press, London. 149.
Mauchly S.J. (1923) Terr. Magn. Atmos. Elect. **28**, 61.
Mühleisen R. (1956) J. Atmos. Terr. Phys. **8**, 146.
Mühleisen R. (1958) *Recent Advances in Atmospheric Electricity*. Pergamon Press, London. 213.
Ogawa T. (1960a) J. Geomag. Geoelect. **11**, 139.
Ogawa T. (1960b) J. Geomag. Geoelect. **11**, 165.
Sagalyn R.C. and Faucher G.A. (1956) Quart. J.R. Met. Soc. **82**, 428.
Sapsford H.B. (1936) Terr. Magn. Atmos. Elect. **41**, 29.
Yokouti S. (1938) Memoirs Kakioka Magn. Observ. **1**, 1 (in Japanese).

The Cosmic Ray Equator and the Geomagnetism

By Kunitomo SAKURAI

Geophysical Institute, Kyoto University

(Read October 17, 1959; Received July 1, 1960)

Abstract

It was temporarily thought that the disagreement of the position of geomagnetic dipole equator with that of the cosmic ray equator would be caused by 45° westward shifting of the latter. At first, we examine, referring to the theory of geomagnetic effect on cosmic rays, whether such westward shifting can be existent or not. It is shown, in view of this examination, that the deviation of the cosmic ray equator from the geomagnetic dipole equator is negligible even if the magnetic cavity is present around the earth's outer atmosphere. Taking into account such results, we investigate the origin of the cosmic ray equator and show that this equator can be produced by the higher harmonic components combined with the dipole component of geomagnetism. We then consider the relation of the origin of the cosmic ray equator to the eccentric dipoles, near the outer part of the earth's core, contributing to the secular variation of geomagnetism.

1. Introduction

Since disagreement of the so-called cosmic ray equator with the geomagnetic eccentric dipole equator was made clear by Simpson, Fenton, Katzman and Rose (1956), theoretical studies which extend the theory of geomagnetic effect on cosmic rays to the case including higher harmonic components of geomagnetism, and the investigations on the relation of the cosmic ray equator to the magnetic dip equator have been performed. On the other hand, the investigation on the physical state of the earth's outer atmosphere made clear that the geomagnetic field does not extend to infinite distance from the earth, but is restricted within the sphere of about 10 earth radii, taking the earth as center, the so-called magnetic cavity being formed in the space around the earth (Dungey, 1955). And then, the observation of the geomagnetic field by the earth satellite Pioneer I shows that this magnetic cavity is, in fact, formed near the position of 10 and several earth radii (Sonett, Judge and Kelso, 1959). If such magnetic cavity exists in the outer fringe of the earth's outer atmosphere, conventional results from the theory of geomagnetic effect on cosmic rays will be obliged to suffer some alteration. We, therefore, think that it is necessary to examine whether this alteration is necessary or not. Accordingly, in this paper we shall examine in section 2 the orbits of cosmic ray particles in the geomagnetic dipole field. Next, we shall consider in section 3 the origin of the cosmic ray equator, referring to the results from section 2 and studies on the cosmic ray equator so far presented.

2. Results from the Motion of Cosmic Ray Particles in the Geomagnetic Field

Theoretical studies on the geomagnetic effect on cosmic rays considering higher harmonic terms of geomagnetic field and on the cosmic ray equator deduced from that theory were done by Jory (1956) and by Kellogg and Schwartz (1959). In particular, the studies by Kellogg and Schwartz (1959) show that the position of the cosmic ray equator agrees considerably with the theoretical one. In these studies, however, they took into account the higher harmonics of geomagnetic field, but did not consider that the extension of geomagnetic field was finite, that is to say, they treated the case of absence of magnetic cavity around the earth. Taking into account the fruit from the studies on the earth's outer atmosphere, we, therefore, think that it is necessary to examine again the theory of geomagnetic effect on cosmic rays. Since it is in fact very difficult to do the calculation, we shall calculate the motion of cosmic ray particles in the geomagnetic equatorial plane: namely, we are going to examine to what extent the alteration will be which orbits of cosmic ray particles suffer as the result of the existence of magnetic cavity. We shall restrict this calculation in the case of the geomagnetic equatorial plane alone because it is impossible to integrate analytically the equations of motion of cosmic ray particles except for the equation in the equatorial plane. Although we cannot expect fruitful results from this calculation, it is possible to estimate a limit for alteration of conventional theory of geomagnetic effect and to get other clue to 45° westward shifting of cosmic ray equator from the geomagnetic dipole equator obtained by Simpson, Fenton, Katzman and Rose (1956). Since we restrict the calculation on the motion of cosmic rays in the equatorial plane of geomagnetic dipole field, we are able to integrate analytically the equations of motion, as was already performed by Vallarta, Graeff and Kusaka (1939), Jánossy (1950) and Störmer (1955), and accordingly we are able to proceed further our discussion on the cosmic ray particle orbits in view of these results. In the next place, we shall consider the properties of magnetic cavity around the earth. Both of theoretical study on the earth's outer atmosphere (Dungey, 1955; 1958) and of the analysis of observational data from the earth satellite Pioneer I (Sonett, Judge and Kelso, 1959) show that the extension of geomagnetic field is confined within the sphere of 6 to 15 earth radii and that outside this sphere its form is not dipole type while within the sphere the dipole magnetic field extends as it stands. Hence, the dimensions of magnetic cavity range from 6 to 15 earth radii. Because the analysis by Sonett et al. (1959) makes clear the extension of geomagnetic field to be confined within the sphere of 13 to 15 earth radii, it will be safe to say that outside this sphere cosmic ray particles do not receive the influence of geomagnetism. We shall, therefore, consider the motion of cosmic ray particles inside the magnetic cavity.

As the calculation of orbits of vertically incident cosmic ray particles to the earth in the geomagnetic equatorial plane was done by Jory (1956) and Lüst (1957), we can compare the orbits of cosmic ray particles in the existence of magnetic cavity with their results. If we know the degrees of discrepancy between the directions of asympto-

tic vectors by Jory (1956) and Lüst (1957) and the directions of velocity vectors of a negative particle at the time when it, after ejected from the earth vertically, arrives at the surface of magnetic cavity, we can estimate the orders of magnitude of effect of the existence of magnetic cavity on the motion of cosmic ray particles. We here take into account studies by Dungey (1955), Tamao (1959) and by Sonett, Judge and Kelso (1959) and others, but, for simplicity, we shall assume the magnitude of extension of equatorial plane of geomagnetic dipole equator, i.e. dimension of magnetic cavity, as 10 earth radii. The directions of velocity vectors of cosmic ray particles at the position of magnetic cavity calculated on the basis of the above assumption are shown as $(\lambda_{10}, \varphi_{10})$; latitude component and longitudinal one, respectively, of velocity vectors. It is now easy to compare the asymptotic velocity vectors $(\lambda_\infty, \varphi_\infty)$ by Jory (1956) and Lüst (1957) with them. Since the range being treated now is confined in the geomagnetic equatorial plane, there is $\lambda_{10}=\lambda_\infty=0$. We show in Fig. 1 the calculated results on both of φ_{10} and φ_∞ with respect to particle rigidities. An evidence

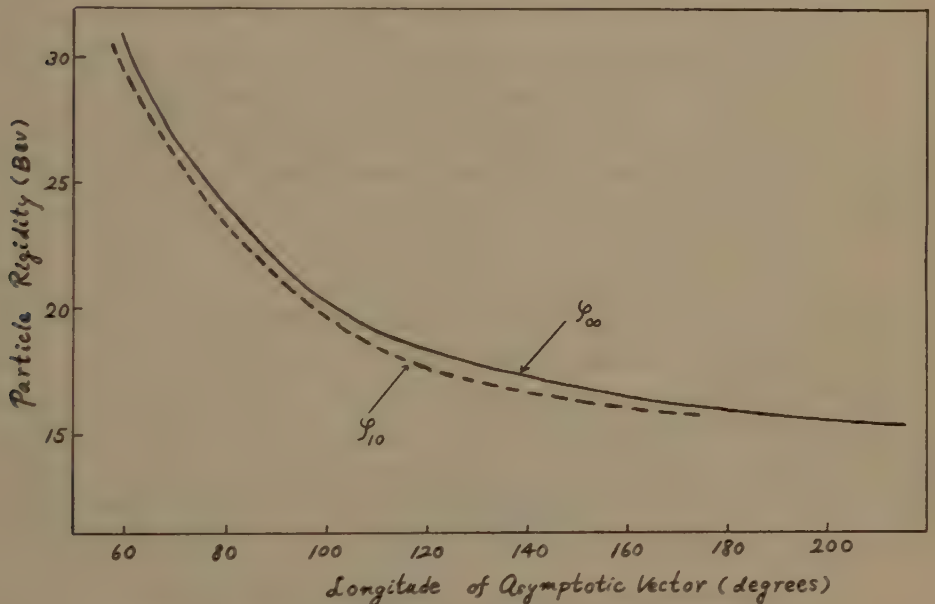

Fig. 1. φ_{10} and φ_∞ with respect to particle rigidity.

from the above calculation is that the conventional results from the theory of geomagnetic effect on cosmic ray receive negligible alteration at most because we can show that the westward shifting of the cosmic ray equator is only several degrees in longitude even if the magnetic cavity is existent. We can, therefore, conclude that the cosmic ray equator is not produced by the interaction of the magnetic field in the earth's outer atmosphere with the interplanetary plasma. Accordingly, it is not reasonable to say that the cosmic ray equator is shifted westward by 45° from the geomagnetic dipole equator so long as we admit the existence of magnetic cavity in the earth's outer atmosphere. Since it has been shown that the geomagnetic field and

plasma within magnetic cavity rotate rigidly with the earth (Dungey, 1958), there is no possibility that the magnetic field within this magnetic cavity is dragged westward. If there is such dragging, the cosmic ray equator will be equivalent to the equator formed by 45° westward shifting of geomagnetic dipole equator itself, but, as this consideration is inconsistent with the observation, we cannot adopt it. Moreover, if whole geomagnetic field in the outer atmosphere above the ionosphere is dragged, it will be possible to explain 45° westward shifting of cosmic ray equator, but we must seek other explanation for the cosmic ray equator because we can adopt such explanation neither theoretically nor experimentally. On the other hand, although it seems, as Maeda (1957) and Tamao (1957) considered, that the geomagnetic field extending outside magnetic cavity is perhaps dragged or disturbed, as a result of the earth's rotation, by its interaction with plasma in the interplanetary space, it will be obvious from the above calculation that the orbits of cosmic ray particles are hardly altered by this interaction. It is, therefore, not possible to explain the origin of the cosmic ray equator from the view point of their considerations. We have examined the motion of cosmic ray particles in the equatorial plane until now, but, as it is difficult to calculate the orbits of cosmic ray particles in general, we shall not do this calculation here. However, as Sandström (1958) says, it will, in general, be possible to think that the existence of magnetic cavity in the space around the earth is hardly influent on conventional theory of geomagnetic effect on cosmic rays. The results in this section may also show that the above estimation is admissible. Hence, we cannot take part with the conclusion that the cosmic ray equator is made by the westward shifting of geomagnetic field. The origin of the cosmic ray equator is not the westward drag of geomagnetic field in the outer atmosphere by the interplanetary plasma, and therefore, we can conclude that this cause is in the interior of the earth, or in unusual phenomena within magnetic cavity. Since, in view of the above results, the conventional theory of geomagnetic effect on cosmic rays hardly receive the alteration by the existence of magnetic cavity, it is sufficiently reliable to conclude that the results of the geomagnetic effect in the case of higher harmonic components of geomagnetism obtained by many authors, are also hardly altered.

3. Discussions on the Origin of the Cosmic Ray Equator

In section 2, we showed in view of the geomagnetic effect on cosmic rays that conclusion that the cosmic ray equator shifted westward by 45° from the geomagnetic dipole equator (Simpson, Fenton, Katzman and Rose, 1956) was not true. Afterwards, while many workers have reexamined whether or not the geomagnetic dipole field was shifted westward in the earth's outer atmosphere, the fact that the cosmic ray equator coincides considerably with the magnetic dip equator has been made clear by many authors (Rothwell, 1958; Rothwell and Quenby, 1958; Zmuda, 1958; Kellogg and Schwartz, 1959; Storey, 1959). Although the cosmic ray equator accords well with the magnetic dip equator, it has no such tendency with respect to the geomagnetic dipole equator. This fact, therefore, perhaps shows the influence of geomagnetic higher harmonic com-

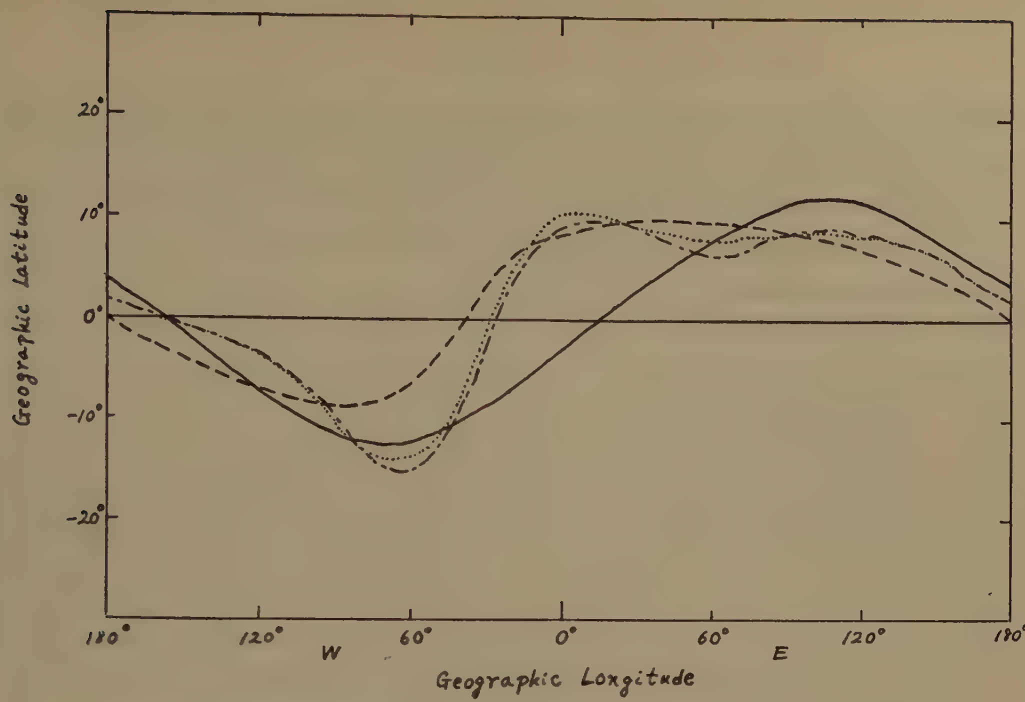

Fig. 2. Various equators.
(a) Comparisons of cosmic ray equator with equators of geomagnetism.
——— Geomagnetic eccentric dipole equator.
— — — Cosmic ray equator.
— - — - Dip equator for 1945 (after Vestine et al., 1947).
········ Dip equator for 1955 (after Finch et al., 1955).

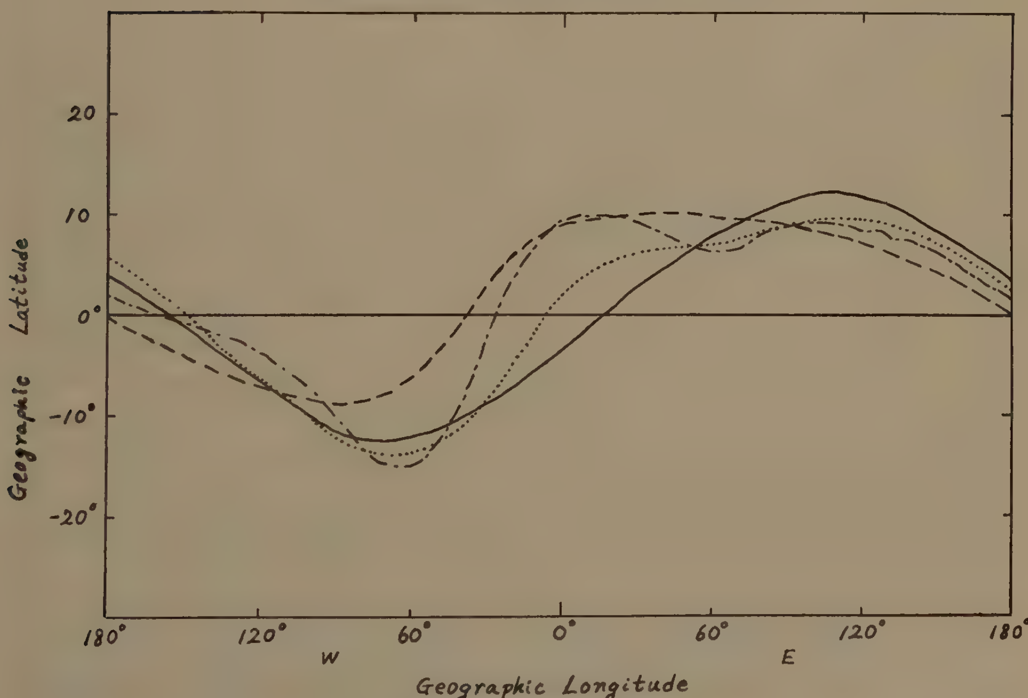

(b) Cosmic ray equator and Geomagnetic equators.
——— Geomagnetic eccentric dipole equator.
— — — Cosmic ray equator.
— - — - Surface magnetic equator involving higher order harmonics (after Vestine et al., 1947). (This is equivalent to dip equator.)
········ Geomagnetic equator at 5000 km above the earth's surface (after Vestine et al., 1947).

ponents upon the motion of cosmic rays is very large. Accordingly, we shall at first compare the geomagnetic equator including higher harmonic components, i.e. geomagnetic intensity minimum line, with the cosmic ray equator. And then, in order to see how far from the earth such higher harmonic components are effective, we shall also compare the cosmic ray equator with the geomagnetic intensity minimum line at height 5000 km above the earth. The results of these comparisons are shown in Fig. 2. The geomagnetic data used here for these comparisons are those published by Vestine, Laporte, Lange and Scott (1947) and by Finch and Leaton (1957).

It is obvious from Fig. 2 that the cosmic ray equator coincides considerably well with the geomagnetic intensity minimum line. Hence, the conclusion that cosmic ray equator coincides with the magnetic dip equator as made clear by Rothwell (1958) will be correct. The observation by Katzman, Meyer and Simpson (1958) also shows similar results as the above conclusion. Further, Kodama (1959) analyzed the world-wide distribution of cosmic ray neutron intensity at sea level and showed that the cosmic ray equator was different from the one which was calculated strictly by Kodama, Kondo and Wada (1957). This result also shows that the cosmic ray equator is made by some cause other than the dipole component of geomagnetism. Thus, both facts that the cosmic ray equator coincides very well with the magnetic dip equator and that the geomagnetic equator including higher harmonic components shows similarly well accordance with the cosmic ray equator (Fig. 2) give support to theoretical investigation by Kellogg and Schwartz (1959). These results clearly show that the origin of cosmic ray equator is situated in the interior of the earth. Although it was once presented (Simpson, Jory and Pyka, 1956) that the origin of the cosmic ray equator is magnetic anomalies in the earth's interior, it is evident from the studies by Nagata (1942) and Zmuda (1958) that the extension of magnetic anomalies in the earth's crust is very localized and therefore they can hardly affect the motion of cosmic rays. In consequence, we can conclude that the origin of the cosmic ray equator is situated deep in the interior, i.e. in the core, of the earth. The studies concerning the secular variation of geomagnetic main field show that the cause of this secular variation is able to explain by means of several eccentric dipoles near the outer part of the earth's core (Bullard, 1948; Lowes and Runcorn, 1951; Runcorn, 1956). Further, these studies made clear that these eccentric dipoles have the moments with radial directions with respect to the earth center and lie in the outer part of the core with outward or inward directions, and the magnitudes of these dipoles are about ten times smaller than the magnitude of geomagnetic main dipole moment. If these eccentric dipoles cause the secular variation and anomalies of geomagnetism, we can suppose that they will affect considerably the motion of cosmic ray particles. Since, if higher harmonic components are included in the analysis of geomagnetism, the components of these eccentric dipole fields are also included, it will be perhaps supposed that there are some relations between the positions of these eccentric dipoles and those of the cosmic ray equator. From the above consideration, we shall show in Fig. 3 the positions of eccentric dipoles

and of the cosmic ray equator. It will be possible to find out some relations between cosmic ray equator and eccentric dipoles. Throughout these considerations, we could make clear that the origin of the cosmic ray equator is situated deep in the interior

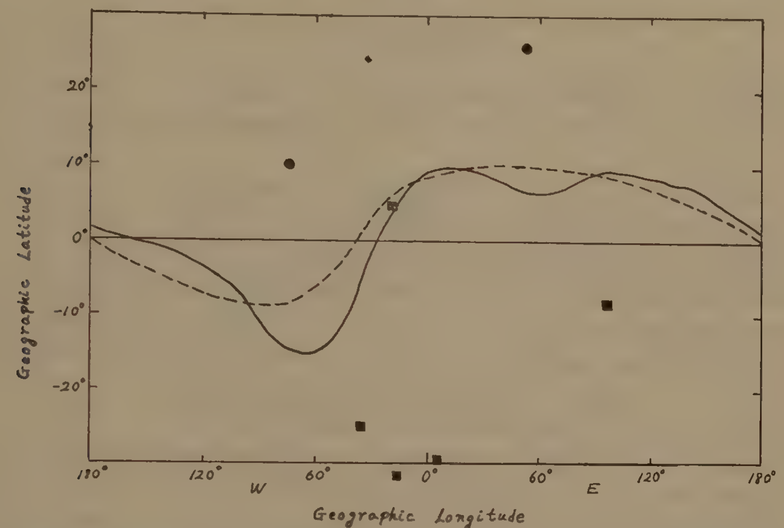

Fig. 3. Cosmic ray equator and the eccentric dipoles contributing to magnetic anomalies.

● : A dipole directed radially inward.

■ : A dipole directed radially outward.

of the earth and perhaps lies in the higher harmonic components of geomagnetism. But, as examined in section 2, in order to obtain these results, we took into account that the magnetic cavity is existent in the earth's outer atmosphere and rotates rigidly with the earth. As it is made clear that the origin of maximum line of geomagnetic diurnal variation is related to the position of magnetic dip equator (Hirono, 1952), the study on the relation of the cosmic ray equator with the maximum line of geomagnetic diurnal variation (Oguchi and Kodama 1959) may also show that the origin of the cosmic ray equator is situated in the interior of the earth.

4. Conclusion

In section 2, we showed that, when the magnetic cavity is existent in the outer atmosphere, such conclusion that Simpson, Fenton, Katzman and Rose (1956) attained could not be derived. And then, in section 3, taking into account the above conclusion, we considered on the origin of the cosmic ray equator and made clear that the cosmic ray equator is made by influence of higher harmonic components of geomagnetism extending within the magnetic cavity. The origin of the cosmic ray equator will be, therefore, situated in the interior of the earth. It is, moreover, impossible to regard the local magnetic anomalies in the earth's crust as a origin of cosmic ray equator. In consequence, we shall suggest that the origin of the cosmic ray equator may lie in the eccentric dipoles, in the outer part of the earth's core, contributing to the geomagnetic secular variation.

Acknowledgement

The author wishes to express his sincere thanks to Prof. Y. Tamura and Prof. M. Hasegawa for their kind advice and continued interest throughout this work.

References

Bullard E.C. (1948) M.N. Geophys. Suppl. **5**, 248.

Dungey D.W. (1955) Rep. Phys. Soc. Conf. on Phys. of Ionosphere at Cavendish Lab. Cambridge, Sep, 1954.

Dungey D.W. (1958) Cosmic Electrodynamics; Cambridge Univ. Press.

Finch H.F. and Leaton B.R. (1957) M.N. Geophys. Suppl. **7**, 314.

Hirono M. (1952) J. Geomag. Geoel. **4**, 7.

Jánossy L. (1950) Cosmic Rays, 2nd ed.; Oxford Clarendon Press.

Jory F.S. (1956) Phys. Rev. **102**, 1167.

Jory F.S. (1956) Phys. Rev. **103**, 1068.

Katz L., Meyer P. and Simpson J.A. (1958) Nuovo Cim. Suppl. **8**, 277.

Kellogg P.J. and Schwartz M. (1959) Nuovo Cim. **13**, 761.

Kodama M., Kondo I. and Wada M. (1957) J. Sci. Res. Inst. **51**, 138.

Kodama M. (1959) J. Geomag. Geoel. **10**, 37.

Lowes F.J. and Runcorn S.K. (1951) Phil. Trans. **A243**, 525.

Lüst R. (1957) Phys. Rev. **105**, 1827.

Maeda K. (1957) Rep. Ionos. Res. Japan **11**, 116.

Nagata T. (1942) Bull. Earthqu. Res. Inst. **20**, 107.

Oguchi T. and Kodama M. (1959) Nature **183**, 103.

Rothwell P. (1958) Phil. Mag. **3**, 961.

Rothwell P. and Quenby J. (1958) Nuovo Cim. Suppl. **8**, 249.

Runcorn S.K. (1956) The magnetization of the Earth's Body, Hd. der Phys. **67**, 498.

Sandström A.E. (1958) Ark. för Fys. **14**, 409.

Simpson J.A., Fenton K.B., Katzman J. and Rose D.C. (1956) Phys. Rev. **102**, 1648.

Simpson J.A., Jory F.S. and Pyka M. (1956) J. Geophys. Res. **61**, 11.

Sonett C.P., Judge D.L. and Kelso J.M. (1959) J. Geophys. Res. **64**, 941.

Storey J.R. (1959) Phys. Rev. **113**, 297.

Störmer C. (1955) Polar Aurora; Oxford Clarendon Press.

Tamao T. (1957) Sci. Rep. Tohoku Univ. Geophys. **9**, 1.

Tamao T. (1959) J. Geomag. Geoel. **10**, 143.

Vallarta M.S., Graeff C. and Kusaka S. (1939) Phys. Rev. **55**, 1.

Vestine E.H., Laporte L., Lange I. and Scott W.E. (1947) The Geomagnetic Field, Its Description and Analysis; Carnegie Institution of Washington Publ. No. 580, Washington D.C.

Zmuda A.J. (1958) J. Geophys. Res. **63**, 477.

Electricity in Rain

By Toshio OGAWA

Geophysical Institute, Kyoto University

(Read October 15, 1959; Received July 19, 1960)

Abstract

The continuous observations of the rain current (i), the rate of rainfall (R') and the potential gradient (P) were made. Providing the Wilson's theory of ion capture by water drops, the quantitative representation between them is obtained using the size-distribution of raindrops by Marshall and Palmer as

$$i=2.12\times10^{-6}P_h R'^{0.84}-0.54\times10^{-6}P_h R'^{1.05},$$

where $\bar{i}$ gives the maximum rain current and P_h is the potential gradient in the charging region of raindrops below the clouds. Applying the calculated result to the measured ones, it is found that P_h relates to P by $|P_h|=3P^{1.3}$. The relation between the above results and the Simpson's empirical ones is discussed. Further, some results in regard to the splashing effect of raindrops at the ground and to the mirror-image effect between the rain current and the potential gradient are described.

1. Introduction

The relationship between the rain current (i esu/cm² sec), the rate of rainfall (R' mm/hr) and the atmospheric electric potential gradient (P V/cm) or the point discharge current (I esu/sec) were investigated in detail by Simpson (1949) who obtained the following empirical formulae

$$\frac{i}{I}=2.0\times10^{-8}R'^{0.57} \tag{1}$$

when the potential gradient is greater than $|20|$ V/cm, and

$$i=-0.040\times10^{-5}(P-4)R' \tag{2}$$

when the potential gradient is smaller than $|10|$ V/cm.

Best (1953) has shown that the non-linearity of the relation between the rain current and the rate of rainfall is explained by the drop-size distribution $F=1-\exp[-(x/a)^n]$ which was obtained by himself (Best, 1950a), where F is the fraction of liquid water in the air comprised by drops with diameter less than any diameter of x, and a and n are constants. He has shown in the expression of rain current $i=C\,(R')^r$ that r has a value which differs very little from 0.73, where C is the value including the potential gradient. He was not concerned with the absolute magnitude of i but only with the variation of i as R' varies. Accordingly the values of C were of little interest.

The purpose of this paper is to show the quantitative expression between the rain current, the rate of rainfall and the potential gradient, and to compare the result with the observed one.

2. Rain Current

The rain current i is given by the general relation

$$i=\int_0^\infty NQVdx, \tag{3}$$

where N is the number of raindrops in unit volume of space, Q the charge on drops and V the velocity of drops, all of which are the functions of the diameter of drop, x.

For the number of raindrops is applied the distribution with size by Marshall and Palmer (1948) in the original form $N_D=N_0e^{-\Lambda D}$, where D is the diameter, $N_D\delta D$ is the number of drops of diameter between D and $D+\delta D$ in unit volume of space, and N_0 is the value of N_D for $D=0$. It is found that $N_0=0.08\,\mathrm{cm}^{-4}$ for any intensity of rainfall, and that $\Lambda=41R'^{-0.21}\,\mathrm{cm}^{-1}$. Accordingly, the above relation is expressed with the present system of units by

$$N=0.008\exp[-4.1R'^{-0.21}x], \tag{4}$$

where x is the drop diameter measured in mm.

The Wilson's theory of ion capture by water drops (Wilson, 1929) is applied for the final charges of raindrops. The final charge of raindrop falling through a region of the potential gradient X is supposed following the calculations of Whipple and Chalmers (1944) as $Q=-3Xa^2$, where Q gives the maximum charge in esu per drop, X the electric field in esu and a the radius of a raindrop in cm. This is expressed with the present system of units and notations as

$$Q=-2.5\times10^{-5}P_hx^2, \tag{5}$$

where P_h represents the potential gradient in V/cm in the charging region of raindrops.

The terminal velocity of raindrops falling through the atmosphere was given by Best (1950b) as $V=A\exp bz\,\{1-\exp[-(d/a)^n]\}$, where A, b, a and n are constants. V is measured in cm/sec, z (the height) in km and d (the drop diameter) in mm. Using the values of constants for the Summer Tropical atmosphere presented in his paper, the above formula can be approximated with the present system of units and notations to

$$V=958\{1-\exp[-0.52x^{1.147}]\}. \tag{6}$$

This is over estimated in the value of some 2% than in the case of the I.C.A.N. standard atmosphere.

Using Eqs. (4), (5) and (6), the maximum electric current carried down by raindrops becomes from Eq. (3)

$$i=-1.915\times10^{-4}P_h\int_0^\infty x^2\exp[-4.1R'^{-0.21}x]\{1-\exp[-0.52x^{1.147}]\}dx. \tag{7}$$

When x is substituted for $x^{1.147}$ in the last term of Eq. (7) the above integrand can be integrated, and Eq. (7) can be written approximately thus

$$i = -2.12\times10^{-6}P_h R'^{0.84} + 0.54\times10^{-6}P_h R'^{1.05}\,; \qquad (8)$$

it results in the less estimation of about 5% within the actual range of raindrop diameter x. Eq. (8) is graphically expressed with logarithmic scale by Fig. 1, in which the curve is almost straight in the range of smaller values of R'.

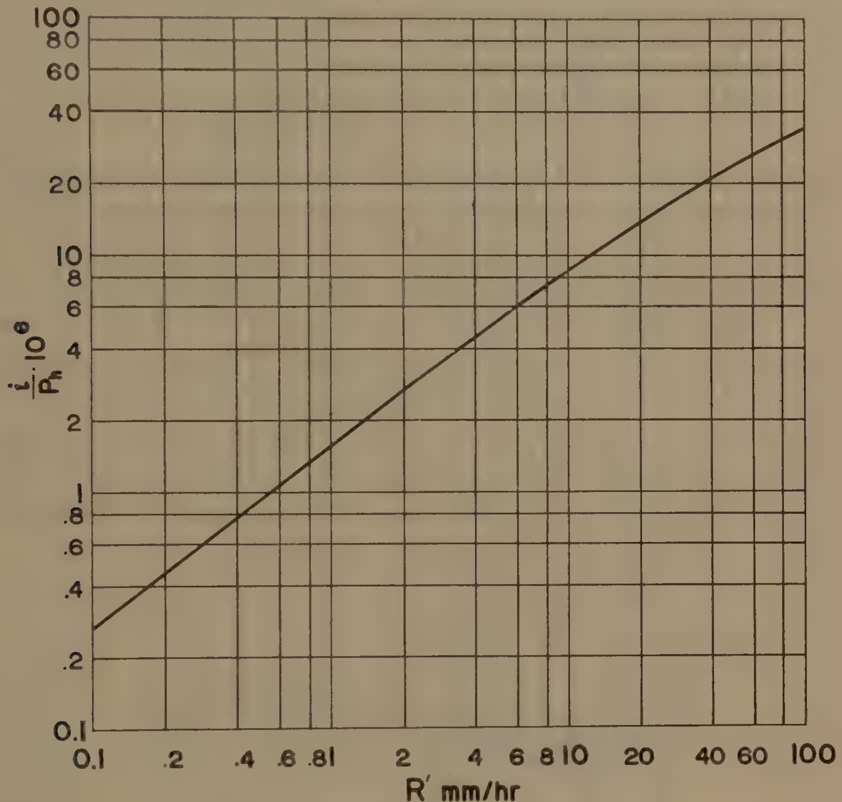

Fig. 1. Relation between rain current (i), rate of rainfall (R') and potential gradient in charging region (P_h) given by Eq. (8).

3. Potential Gradients below Clouds

There is a very striking discrepancy about the values of the potential gradient below the clouds. That is, the calculations by Whipple and Scrase (1936), using the theory of Wilson (1925), give the expected values of the considerably greater potential gradient produced by the considerable space charge due to point discharge below clouds. While, the measurements of the potential gradient using the altielectrograph (Simpson and Scrase, 1937; Simpson and Robinson, 1940) show little, if any, increase of potential gradient with height below clouds. In order to remove the discrepancy between the calculated potential gradients and the measured ones, Chalmers (1939) has considered the negative ions coming from the clould and also (Chalmers, 1944) the charges of raindrops or vertical air currents to decrease the space charge, but could not remove it. Thus, there has been no conclusive solution of this serious problem until today.

It is, horeupon, a pressing need to get more knowledges of the potential gradient

actually existing below clouds. Hutchinson and Chalmers (1951) found, from the measurements of the charge and the radius of raindrops and the potential gradient, that raindrops must have fallen through fields several times larger than those at the ground. Smith (1955), also from the measurements of the electricity on individual drops of rain, got the potential gradients in the charging region from $330\,V/\text{cm}$ to $3{,}000\,V/\text{cm}$ corresponding to the values at the ground from $21\,V/\text{cm}$ to $78\,V/\text{cm}$. Their results thus support the existence of the space charge of ions from point discharge, but as to the magnitude of the potential gradient in the charging region, it requires further exami nation.

If the rain current and the rate of rainfall are measured, the minimum values of potential gradients in the charging region can be estimated by using Eq. (8). Since February, 1959 the continuous measurements of the rain current, the rate of rainfall and the potential gradient have been made at the Geophysical Institute of Kyoto University. The rain electrograph used here is similar to that of Simpson (1949) and the d.c. amplifier is used instead of the electrometer. The electrical capacity of the receiver is equal to 109 cm and the area of the mouth of the cone $78.6\,\text{cm}^2$.

The rain current and the potential gradient in showers, in general, change sign very frequently. The record of the typical example on August 12, 1959 is reproduced in Fig. 2. Some considerations as to the mirror-image effect will be made later. This

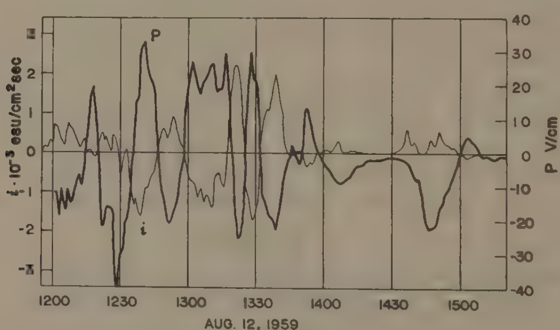

Fig. 2. Reproduction of record showing mirror-image effect between rain current (i) and potential gradient (P) on Aug. 12, 1959.

shower continued from 1040 to 1510 and there occurred lightnings at a long distance during the period from 1140 to 1240. By using the data every one minute from 1200 to 1507 the minimum values of potential gradients in the charging region were calculated from Eq. (8). The results thus obtained are plotted in logarithmic scale in Fig. 3 against the potential gradients measured at the ground except during the short period when the sign is changing. It will be noticed that the points are roughly distributed on a line which is represented by

$$|P_h| = 3P^{1.3}\,. \tag{9}$$

The another typical example was obtained on August 13–14, 1959 when, after the intermittent thunder-showers during the period from 1200 to 1800 on August 13, the

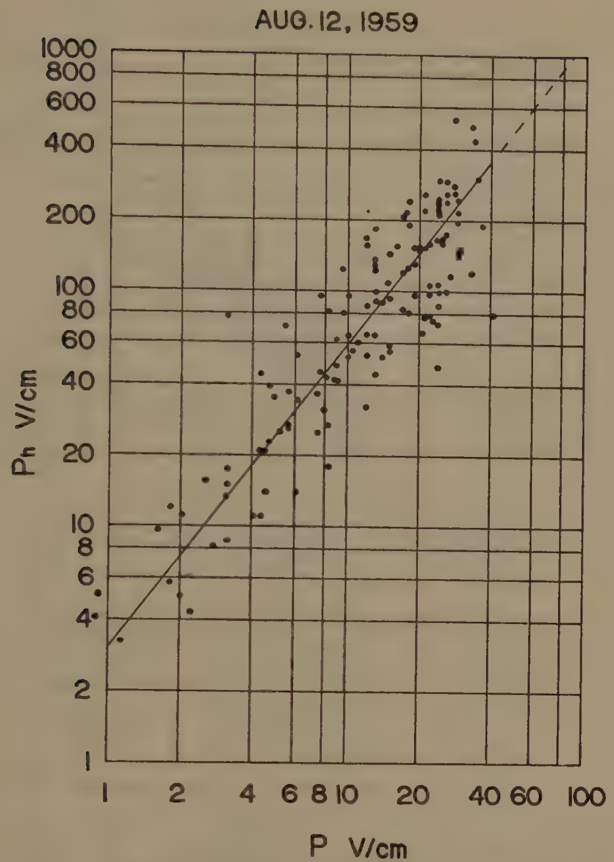

Fig. 3. Relation between potential gradients in charging region (P_h) and those at ground (P), plotted from measurements on Aug. 12, 1959.

potential gradient had continued to have the negative value until 0050 on August 14. Fig. 4 is a reproduction of the record from 2300 on August 13 to 0534 on August 14. The calculated values of the minimum potential gradients in the charging region are

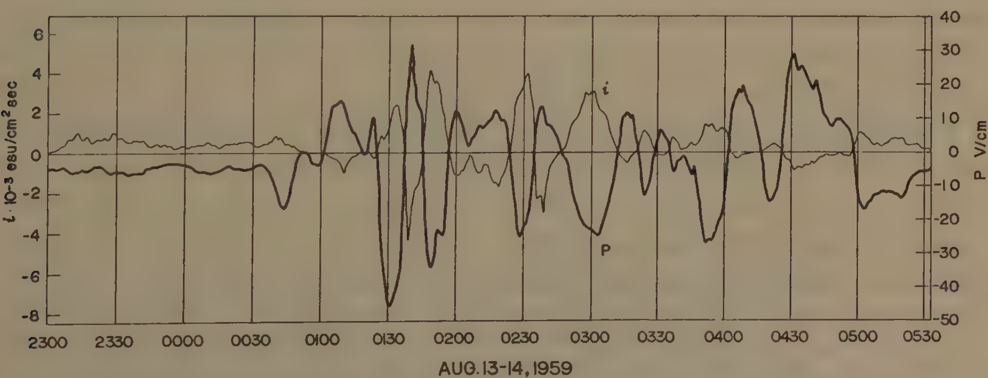

Fig. 4. Reproduction of record showing mirror-image effect between rain current (i) and potential gradient (P) on Aug. 13–14, 1959.

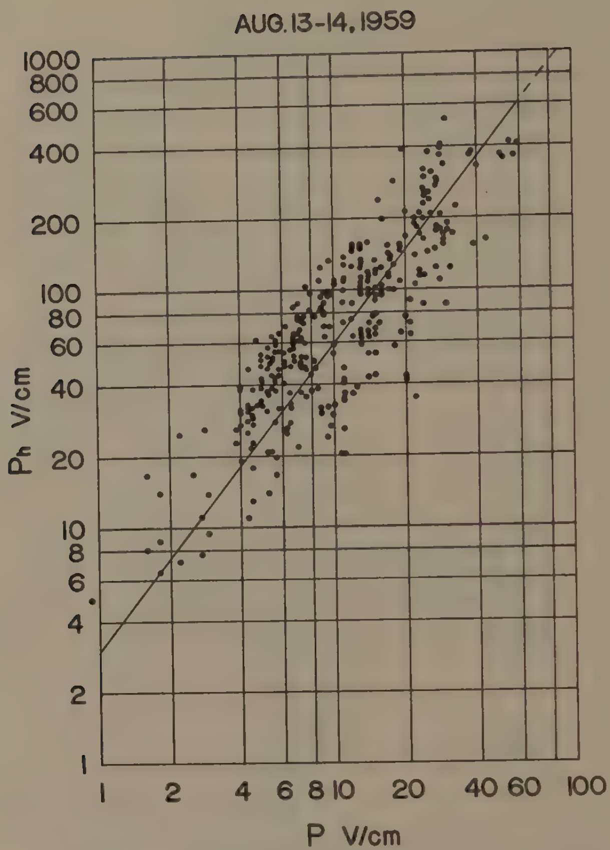

Fig. 5. Relation between potential gradients in charging region (P_h) and those at ground (P), plotted from measurements on Aug. 13–14, 1959.

also plotted in Fig. 5 against the potential gradients at the ground by using the data obtained in Fig. 4. It is a surprising fact that the points in the second example are also distributed near the same line as in the first example. Thus, Eq. (9) gives the relation between the minimum potential gradients in the charging region and the potential gradients at the ground. In the above examples the maximum value of the potentiel gradient measured at the ground was $60\,V/\mathrm{cm}$. Then the relation between the potential gradients at the ground larger than $60\,V/\mathrm{cm}$ and the corresponding potential gradients in the charging region, is not obtained, but it is little supposed that the relation deviates from the above result. It must be noticed that in the above obtained result there is no characteristic which depends on the magnitude of the potential gradient.

Eq. (9) is graphically expressed by Fig. 6. The values of P for the present examples range from $1\,V/\mathrm{cm}$ to $60\,V/\mathrm{cm}$ and the corresponding values of P_h from $3\,V/\mathrm{cm}$ to $600\,V/\mathrm{cm}$. If P is $155\,V/\mathrm{cm}$ which corresponds to the maximum value in Table III of Simpson (1949), P_h becomes $2{,}000\,V/\mathrm{cm}$. These will give appropriate values of the potential gradients in the charging region and support the existence of larger potential gradients below the clouds.

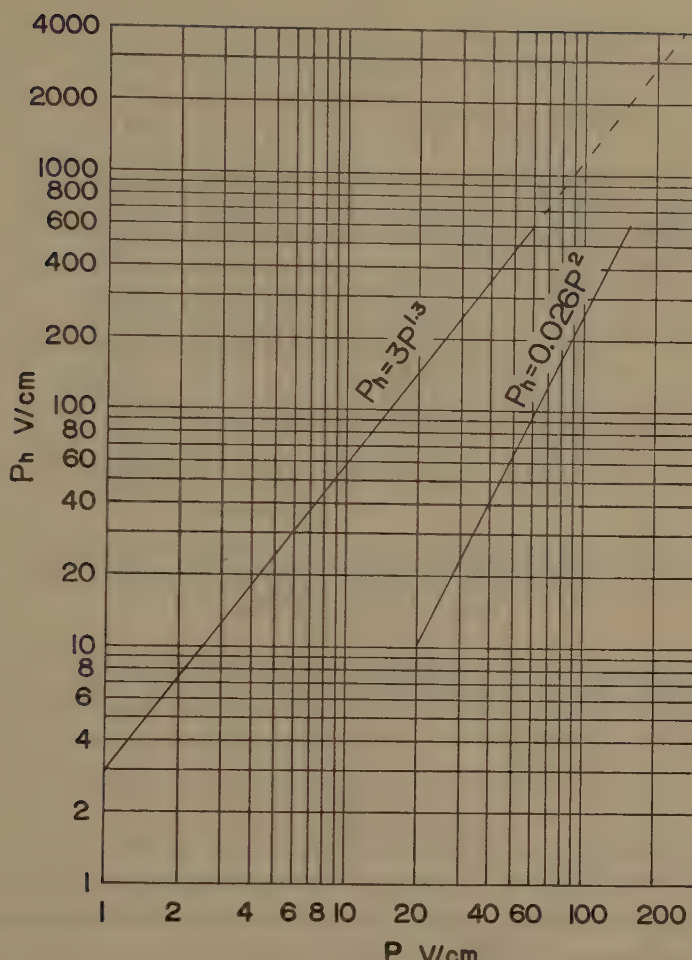

Fig. 6. Relation between potential gradients in charging region (P_h) and those at ground (P), corresponding Eqs. (9) and (13).

4. Comparison with Simpson's formula

In order to compare the above results with Simpson's formula (1), Eq. (8) is approximated from Fig. 1 for the usual rate of rainfall from 1 mm/hr to 50 mm/hr to

$$i=-1.68\times10^{-6}P_hR'^{0.70}. \tag{10}$$

This corresponds to Eq. (1) which is replaced, by the use of the relationship $I=2.7(P^2-8.2^2)$ which was found by Whipple and Scrase (1936), by

$$i=5.4\times10^{-8}P^2R'^{0.57}, \tag{11}$$

where 8.2^2 can be neglected as compared with the values of P^2 for $P>|20|V/\text{cm}$.

Here, the value of the power of R' in Eq. (1) is reexamined. When the values of $\log\left(\frac{10^8}{2}\cdot\frac{i}{I}\right)$ are plotted against $\log R'$ from the data for $P>|20|V/\text{cm}$ (Table III of Simpson, 1949), it may be satisfactorily permissible to give $R'^{0.70}$ instead of $R'^{0.57}$ as shown in Fig. 7. Then Eq. (11) becomes

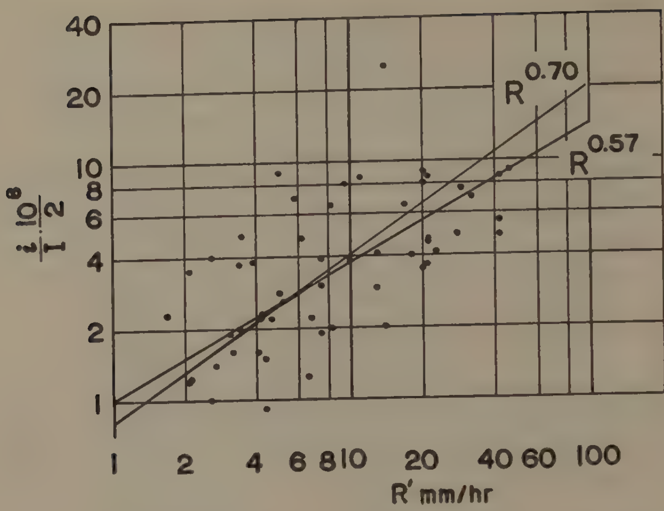

Fig. 7. Relation between rain current (i), rate of rainfall (R') and point discharge current (I), plotted from Table III of Simpson (1949).

$$i=4.32\times10^{-8}P^2R'^{0.70}. \tag{12}$$

From Eqs. (10) and (12)

$$|P_h|=0.026P^2. \tag{13}$$

This gives the relation between the potential gradients in the charging region of raindrops and those at the ground. This is graphically represented in Fig. 6, in which the values of P_h corresponding to those of P from 20 V/cm to 155 V/cm in the data of Simpson can be obtained. When the potential gradient at the ground has the maximum value of 155 V/cm, the potential gradient in the charging region becomes 620 V/cm which is not unexpected value. But the value of P_h is equal to that of P at 38 V/cm and below that value of P, P_h becomes smaller than P. 10 V/cm of the value of P_h corresponds to 20 V/cm of the minimum value of P in the data. It is still a question why the values of P_h are thus smaller than those of P.

5. Effect of Splashing

The effect of the splashing of raindrops at the ground only becomes clear when the value of the potential gradient is small. It occurs usually, however, that the heavy rain is followed by large potential gradients. Accordingly it is very difficult to find an example which shows the effect of splashing of raindrops on the potential gradient. Fig. 8 is a rare example which is thought to show this effect containing the time variations of the potential gradient and the rate of rainfall at 1600–2012 on May 5, 1959. The remarkable isolated minima of the potential gradient at 1800, 1840 and 1922 follow the remarkable isolated maxima of the rate of rainfall at 1751, 1834 and 1918. These phenomena show that the rainfall of 10 mm/hr or more reduces the potential gradient in the value of about 2 V/cm toward negative. Accordingly it will be natural that

the effect of splashing of raindrops should be considered for the rain current when the values of the potential gradient are 10 V/cm or smaller.

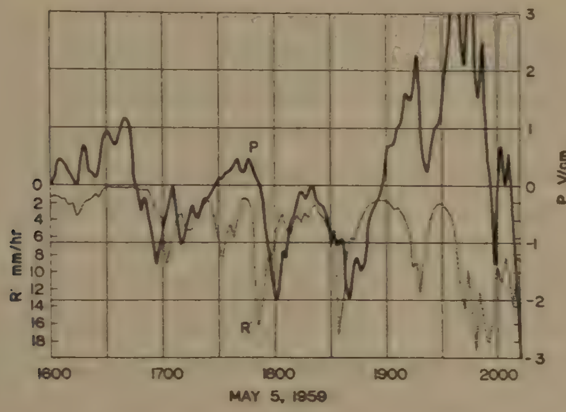

Fig. 8. Reproduction of record showing splashing effect of raindrops on potential gradient (P) on May 5, 1959. R' represents rate of rainfall.

If the amount of charge generated by splashing water is 0.1 esu/cm^3 independent of the electric field (Nolan and Enright, 1922), the positive electric current of $2.8\times10^{-6}R'$ esu/cm^{2}sec flows into the earth by splashing.

While, Simpson's second formula (2) can be replaced by

$$i=-4\times10^{-7}PR'+1.6\times10^{-6}R'. \tag{14}$$

The second term in the right hand side of Eq. (14) is independent of the electric field and may be considered as the positive splashing current to the earth. In fact, Simpson (1949) could not find this effect in snow. The reason why the second term of Eq. (14) is less than the above estimated value of $2.8\times10^{-6}R'$ esu/cm^{2}sec, may be that the funnel-shaped bottom of the rain receiver was less effective than in the case of the flat bottom.

When rain falls in a large potential gradient, small ions of reverse sign to the potential gradient are released in the air by splashing at the ground. This effect can be clearly seen in the records of the polar conductivities. Adkins (1959) discussed the effect of heavy rain on the electric field; small ion production is only due to the induction mechanism. He stated that there is no evidence that the small ions are produced by the Lenard effect independent of the electric field. However, Smith (1955, 1958) showed the effect of negative space charge due to the Lenard effect on the electric field; there must be the process of negative charge production in a small or no electric field.

6. Mirror-Image Effect

The rain current and the potential gradient are usually opposite in sign and they change sign simultaneously, so that the time variation of the rain current appears as

a mirror image of the time variation of the potential gradient.

The mirror-image effect has been found by some workers and not found by others. In order to check up on this matter, the recordes of the rain current and the potential gradient were examined. In the measurements shielding of the rain receiver was very effective—this was proved during the high potential gradient without precipitation—and the smallest drops were not seriouly prevented to fall into the receiver.

Generally, as the mirror-image effect between the rain current and the potential gradient was very remarkable, it was difficult to find out an exception of this effect. Two examples have been shown in Figs. 2 and 4. General results for showers are as follows. (1) In shorter-period variations there is no phase lag between the rain current and the potential gradient. (2) In longer-period variations there is a phase lag between them when the potential gradient has larger values. (3) When there is a phase lag the rain current changes its sign antecedently to the potential gradient. In Table I are shown the results of examination of the points where the rain current and

Table I. Mirror-image effect

	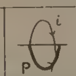	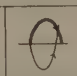	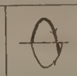	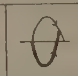	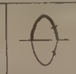	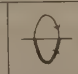	Indistinct
Number of occurrences	11	9	2	1	46		about 60
	20		3				
Average duration of a sign	17 min				10 min		
Average Potential gradient	44 V/cm				26 V/cm		

the potential gradient change sign from typical 18 showers observed in 1959, mainly from June to September. There are about 60 indistinct cases which do not belong to any case. Accordingly the number of occurrences of phase lag is less than 20% of the total number. The delay time is ranged from 1 to 8 min.

7. Concluding Remarks

Some topics in regard to the electricity in rain were mentioned in this paper but little closed discussion has made. For the potential gradients below the clouds, the direct measurement will be the most important key to remove the discrepancy. The splashing effect of raindrops is important in relation to the mechanism of the removal of ions from the splashed water and also to the study of the transient phenomena of ions in the air. The problem of the time lag in the mirror-image effect is related to the mechanism of charging of raindrops. The study is now uninterrupted and further discussions will be made in future.

Acknowledgement

The author wishes to express his sincere thanks to Prof. Y. Tamura for his kind

guidance and encouragement throughout the work. He also wishes to thank Mr. A. Okawati and Mr. S. Saga for their cooperations in the measurements and for their valuable discussions.

References

Adkins C.J. (1959) Quart. J. Roy. Met. Soc. **85**, 237.

Best A.C. (1950a) Quart. J. Roy. Met. Soc. **76**, 16.

Best A.C. (1950b) Quart. J. Roy. Met. Soc. **76**, 302.

Best. A.C. (1953) J. Atmos. Terr. Phys. **3**, 285.

Chalmers J.A. (1939) Quart. J. Roy. Met. Soc. **65**, 237.

Chalmers J.A. (1944) Quart. J. Roy. Met. Soc. **70**, 121.

Hutchinson W.C.A. and Chalmers J.A. (1951) Quart. J. Roy. Met. Soc. **77**, 85.

Marshall J.S. and Palmer W.M. (1948) J. Met. **5**, 165.

Nolan J.J. and Enright J. (1922) Proc. Roy. Dublin Soc. **17**, 1.

Simpson G.C. (1949) Geophys. Mem., London. **84**, 1.

Simpson G.C. and Robinson G.D. (1940) Proc. Roy. Soc. A **177**, 281.

Simpson G.C. and Scrase F.J. (1937) Proc. Roy. Soc. A **161**, 309.

Smith L.G. (1955) Quart. J. Roy. Met. Soc. **81**, 23.

Smith L.G. (1958) Recent Advances in Atmospheric Electricity, Pergamon Press, London. 299.

Whipple F.J.W. and Chalmers J.A. (1944) Quart. J. Roy. Met. Soc. **70**, 103.

Whipple F.J.W. and Scrase F.J. (1936) Geophys. Mem., London. **68**, 1.

Wilson C.T.R. (1925) Proc. Phys. Soc., London. **37**, 32D.

Wilson C.T.R. (1929) J. Franklin Inst. **208**, 1.

Letter to the Editors

The Effect of Proton Gyration in the Outer Atmosphere Represented on the Dispersion Curve of Whistler

(Received June 16, 1960)

Storey (1956) has proposed the influence of proton gyration in the outer atmosphere on the propagation of whistlers especially observed at low geomagnetic latitudes. Whistler waves propagate along the line of geomagnetic force, that will be due to a dipole situated at the center of earth, in the extraordinary mode through the anisotropic and dispersive outer atmosphere. In this paper, a short whistler which is the purest of all ones observed at Kyoto (geomagnetic latitude 24.7°N) during 1958 and fairly well defined to frequencies below 1 kc/s, is analysed for the purpose of detecting the effect of proton gyration on the whistler dispersion.

The group refractive index for the extraordinary mode in the longitudinal propagation is approximately given by $\mu' = \frac{\partial}{\partial f}(\mu f) \simeq \frac{1}{2}\mu = \frac{1}{2}\frac{f_0}{\sqrt{f \cdot f_H}}$ (Storey, 1953), where μ is the wave refractive index, under conditions that both the electron gyrofrequency f_H and the electron plasma frequency f_0 are much greater than the wave frequency f everywhere along the path of propagation and that the motion of positive ions in the electric field of waves and the mean collision frequency in the outer atmosphere are negligible.

The travelling time of whistler is given by $t = \int_{Path} \frac{ds}{V_g}$, where $V_g(=c/\mu')$ is the group velocity, c the velocity of light, and ds the path element. Then the dispersion of whistler, so called the simple law, is given by $tf^{1/2} = \frac{1}{2c}\int \frac{f_0}{\sqrt{f_H}} ds = D$, $f_0^2 = \frac{Ne^2}{\varepsilon_0 \pi m}$, and $f_H = \frac{\mu_0 He}{2\pi m}$, where m is the mass of an electron, e the charge of an electron, N the electron density, H the strength of geomagnetic field and D the dispersion of whistler that is constant for any one path (Storey, 1953). But when the above conditions are not satisfied, the complete dispersion is given by $t \cdot f^{1/2} = \frac{1}{2c}\int \frac{f_0}{\sqrt{f_H}}(1+\delta(f))\, ds$, where the correction term is generally small. At the top of line of force, where both f_H and f_0 are least, the wave frequency becomes primarily comparable to f_H.

i) When f is small compared with f_0 but not small compared with f_H, the group refractive index for the extraordinary mode in the longitudinal propagation is given by $\mu' \simeq \frac{1}{2}\frac{f_0 \cdot f_H}{f^{1/2}(f_H - f)^{3/2}}$ (Helliwell, Pope, Crary, and Smith, 1956). If f dose not approach f_H closely anywhere along the path, the correction factor $\delta_h(f)$ at high audio-frequencies is given by $\delta_h(f) = (1 - f/f_H)^{-3/2} - 1 \simeq 1.5f/f_H + 1.875(f/f_H)^2$. $(f < f_H)$

ii) At wave frequencies not large compared with the ionic gyrofrequency f_i, the

group refractive index for the extraordinary mode in the longitudinal propagation and the correction factor at low audio-frequencies are given by

$$\mu' = \frac{1}{2}\frac{f_0}{\sqrt{f \cdot f_H}}\frac{1+2f_i/f}{(1+f_i/f)^{3/2}}, \quad \delta_l(f) = \frac{1+2f_i/f}{(1+f_i/f)^{3/2}} - 1 \quad \text{and} \quad f_i = \frac{eH\mu_0}{2\pi m_i}$$

respectively, where e is the charge of a proton and m_i is the mass of a proton (Astrom, 1950 and Hines, 1953). Then we obtain the complete dispersion law

$$t \cdot f^{1/2} = \frac{1}{2c}\int \frac{f_0}{\sqrt{f_H}}(1+\delta_h(f)+\delta_l(f))ds = D + \varDelta D_h + \varDelta D_l \quad \text{.........}(1).$$

$\varDelta D_l$ and $\varDelta D_h$ are the departures of dispersion from the simple law at low audio-frequencies and high audio-frequencies respectively.

The proton gyrofrequency at F layer height varies from about 900 c/s at the geomagnetic poles to 450 c/s at the geomagnetic equator and the ionic gyrofrequency of oxygen or nitrogen is quite small in the ionosphere (less than 60 c/s). Therefore we may only consider the effect of prton gyration as that of ionic gyration in the outer atmosphere on the propagation.

The maximum value of $\delta_l(f)$ is 0.0887 at $f=2f_i$. The values of $\delta_l(f)$ are positive for $f > 0.618 f_i$ and negative for $f < 0.618\ f_i$. Considering the variation of $\delta_l(f)$ due to f and the eq. (1), we can see the deviation due to the proton effect from the simple law on the dispersion curve of whistler as Fig. 1.

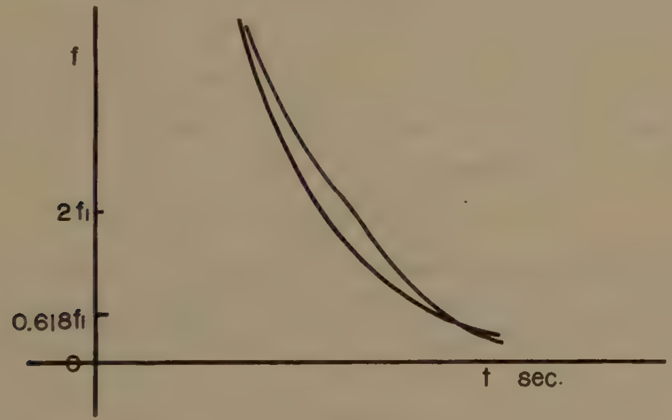

Fig. 1

The proton gyrofrequencies at low heights are greater than those at great heights and the proton effect would appear most markedly in whistlers observed at low latitudes rather than those at high latitudes, because the greater part of the path of whistler observed at the low latitude lies at relatively low heights.

Whistlers observed at low latitudes are suitable for the purpose of detecting the deviation due to the proton gyration from the simple law on the whistler traces, because whistlers observed at high latitudes are generally more spread than those at low latitudes.

Storey (1956) has derived the distribution of electron density in the outer atmos-

phere as $N=600\exp(2.5r_0/r)/\text{cm}^3$, where r is the distance from the center of earth and r_0 is the radius of earth, under the assumption that the outer atmosphere consists of fully ionized hydrogens at a temperature of 1500°K in thermal and hydrostatic equilibrium under gravity and in dynamical equilibrium with the ionization in the interplanetary space (Dungey, 1955).

This distribution gives a value of electron density at 300 km over the ground as $6.8\times10^3/\text{cm}^3$. But this value is much smaller than values of ionospheric observations. Whistlers observed at Kyoto propagate at relatively low heights and go up to the maximum altitude of 1350 km. Therefore we will not adopt Storey's distribution in this case. According to the ionospheric observations, we adopt the parabolic distribution of electron density in the ionosphere.

The propagation path of a whistler observed at Kyoto is conveniently divided into two parts with respect to the altitude and the electron density is constant in each part. In the polar co-ordinate that originates at the center of earth, the dispersion is given by $D=\sqrt{\frac{2er_e^5}{M}}\sqrt{N}\int_0^{\theta_0}\cos^4\theta(1+3\sin^2\theta)^{1/4}\,d\theta$, where r_e is the radial distance from the center of earth at the top of line of force passing through the geomagnetic latitude θ_0 on the earth's surface and M is the earth's magnetic dipole moment. The D layer vanishes generally during the night or in the winter and so we may put the lower limit of the integral (1) at about 100 km over the ground.

i) The part 1 between 100 km and 500 km over the ground.

The constant electron density N_1 in the part 1 is given by $N_1=\frac{1}{400}\int_0^{400}N_m\cdot\frac{2}{Z_m}\left(Z-\frac{Z^2}{2Z_m}\right)dZ$, where N_m is the maximum electron density at the height of Z_m measured from the base of ionosphere that is at 100 km over the ground. The dispersion D_1 caused in the part 1 is given by

$$D_1=\sqrt{\frac{2er_e^5}{M}}\sqrt{N_1}\int_{\theta_{500}}^{\theta_{100}}\cos^4\theta(1+3\sin^2\theta)^{1/4}d\theta.$$

ii) The part 2 between 500 km and 1350 km over the ground that is the top of line of force passing through Kyoto. The constant electron density N_2 in the part 2 is given by $N_2=\frac{M(D-D_1)^2}{2er_e^5}\left|\int_0^{\theta_{500}}\cos^4\theta(1+3\sin^2\theta)^{1/4}d\theta\right|^{-2}$, where D is the total dispersion observed at Kyoto.

In calculating N_m we use the expression $N_m=1.24\times10^{-8}\cdot f_0F_2^2$, where f_0F_2 is the critical frequency in the F_2 layer. f_0F_2 used here is the value at Kokubunzi Radio Research Laboratory (The Radio Research Laboratories in Japan, 1958).

When Kyoto is in the winter, the geomagnetic conjugate point of Kyoto is in the summer. Therefore we had better calculate the dispersion in each hemisphere. For example, $D_{IN}=\frac{1}{2}\sqrt{\frac{2er_e^5}{M}}\sqrt{N_{IN}}\int_{\theta_{500}}^{\theta_{100}}\cos^4\theta(1+3\sin^2\theta)^{1/4}d\theta=2.66\times10^{-2}\sqrt{N_{IN}}\int_{\theta_{500}}^{\theta_{100}}(1-0.15\cos2\theta)d\theta$, where $\theta_{500}=19°31'$ and $\theta_{100}=23°52'$. Instead of the ionospheric values at the conjugate point of Kyoto, we adopt the values at Kokubunzi.

The next table shows the ionospheric values at Kokubunzi in 1958.

	Z_m+100 km	f_0F_2		average	N_m	average
	03h–04h	03h	04h	03h–04h	03h–04h	03h–04h
June	320 km	8.3 Mc/s	8.0 Mc/s	8.15 Mc/s	$8.23\times10^5/\mathrm{cm}^3$	$N_{IS}=6.00\times10^5/\mathrm{cm}^3$
Dec.	300 km	4.1 Mc/s	3.9 Mc/s	4.00 Mc/s	$1.98\times10^5/\mathrm{cm}^3$	$N_{IN}=1.32\times10^5/\mathrm{cm}^3$

From the above table, we can obtain the dispersion in each part as $D_{IS}=8.9\sqrt{s}$, $D_{IN}=4.5\sqrt{s}$, and $D_1=D_{IS}+D_{IN}=13.4\sqrt{s}$. On the other hand, the value of whistler dispersion (24, Dec. 1958, 0335 J.S.T.; Kyoto) is $25.3\sqrt{s}$. Thus we obtain $D_2=11.9\sqrt{s}$ and $N_2=1.42\times10^4/\mathrm{cm}^3$ in the part 2. G. Mck Allcock (1959) has derived the distribution of electron density $N=5.75\times10^4\exp(-h/2640)/\mathrm{cm}^3$ (h in km) between 1000 km and 13000 km over the ground from many whistlers.

According to this distribution, we obtain the electron density in the part 2

$$N=\frac{1}{350}\int_{1000}^{1350}5.75\times10^4\exp(-h/2640)dh=3.89\times10^4/\mathrm{cm}^3.$$

Using the above mentioned value of electron density in each part, we can calculate the complete dispersion.

The term $\frac{1}{2c}\int\frac{f_0}{\sqrt{f_H}}\,\delta_i(f)ds$ in the eq. (1) represents the departure of dispersion from the simple law due to the effect of proton gyration.

The integration in the eq. (1) is numerically performed along the line of force passing through Kyoto. In Fig. 2, the calculated results and the observed values are shown.

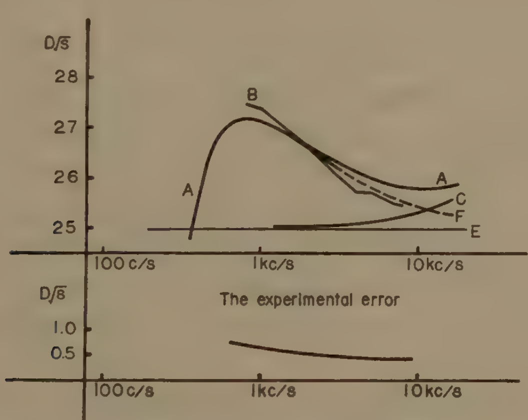

Fig. 2 A: The calculated complete dispersion.
B: The experimental dispersion.
C: The correction at high audio-frequencies due to the effect of electron gyration.
E: Storey's simple dispersion.
F: The correction at low audio-frequencies due to the effect of proton gyration.

It is seen that 'A' agrees roughly with 'B' and that 'B' especially agrees well with 'F'. In other words, the dispersions of whistlers observed at low geomagnetic latitudes are clearly influenced by the effect of proton gyration in the outer atmosphere.

The complete dispersion curve has a minimum point at a frequency above the upper limit frequency observed with our apparatus, while the experimental one does not have it. The complete dispersion curve shows the presence of a maximum point at a frequency below 1 kc/s.

But in Kyoto, the noise level is high and we can not confirm the presence of the maximum point on the experimental dispersion.

Whistlers recorded on the magnetic tapes are analysed with a sonagraph which consists of a number of narrow band filters connected in parallel and tuned to various selected frequencies.

In the physical resonator or the filter consisting of condensers and resisters, defining appropriately the bandwith Δf and the duration of transient phenomenon Δt, we have always the relation $\Delta t \cdot \Delta f \approx 1$ that is due to the uncertainty of wave phenomenon and shows the limit of dynamic measurement (Isobe, 1955).

The tone of whistler used here, is pure and then the frequency f is regarded as the function of time. Δt is represented by the spreadness of whistler trace along the time axis on the sonagram.

We have $f(t+\Delta t) \doteqdot f(t)+df/dt \cdot \Delta t$ and $\Delta f \simeq df/dt \cdot \Delta t$.

Considering the relation $\Delta t \cdot \Delta f \approx 1$ and the dispersion of whistler $t \cdot f^{1/2}=D$, we obtain the expression as $\Delta t \approx |dt/df|^{1/2}=(D/2)^{1/2} f^{-3/4}$.

Thus the experimental error of whistler dispersion is given by $\Delta(t \cdot f^{1/2}) \approx (D/2)^{1/2} \cdot f^{-1/4}$. The experimental error of whistler dispersion (24, Dec. 1958, 0335 J.S.T. ; Kyoto) is shown in the lower part of Fig. 2. The experimental error in this case is below 5% and then we can rely the results of this experiment. Above results agree well with the report by Outsu and Iwai (1959).

It has become clear that whistler observed at Kyoto, where is at low geomagnetic latitude, follows the complete dispersion law given by Storey (1956). In other words, it is certainly able to detect qualitatively the effect of proton gyration in the outer atmosphere by the method adopted here. The missile that was launched from Cape Canaveral on April 7, 1959, reached a maximum altitude of 1230 km and spent about 15 minutes above 1000 km between the latitude of 20°N and 3°N. Freden and White (1959) identified the protons in the outer atmosphere with the nuclear emulsion carried in the missile.

On the other hand, the path of whistler observed at Kyoto goes up to the maximum height of 1350 km. The protons along the path of whistler suggest the presence of radiation zone between about 350 km and 800 km over the ground discovered by Miyazaki and Takeuchi (1959).

Acknowledgements

The authors wish to express his hearty thanks to prof. Y. Tamura for his kind directions and advices, to prof. M. Hasegawa, prof. K. Maeda and prof. M. Ota for their encouragements and supports of this work and also to Mr. I. Kimura for his valuable discussions.

References

Allcock G. Mck (1959) J. Atm. Terr. Phys. **14**, 185.

Astrom E. (1950)Akiv. Fysik. **2**, 443.

Dungey J.W. (1955) The physics of the ionosphere. The Physical Society, London. 229.

Freden S.C. and White R.S. (1959) Phys. Rev. Letters **3**, 9.

Helliwell R.A., Pope J.H., Crary J.H. and Smith R.L. (1956) J. Geophys. Res. **61**, 139.

Hines C.O. (1953) Proc. Cambridge Phil. Soc. **49**, 299.

Isobe T. (1955) Sokutei no Seido. Iwanami Koza (in Japanese) 25.

Miyazaki Y. and Takeuchi H. (1959) Ucyusen Kenkyu **4**, 292.

Outsu J. and Iwai A. (1959) Proc. Res. Inst. Atm. Nagoya Univ. **6**, 44.

Storey L.R.O. (1953) Phil. Trans. Roy. Soc. **A 246**, 113.

Storey L.R.O. (1956) Canadian J. Phys. **34**, 1153.

The Radio Research Laboratories (1958) Ionospheric data in Japan. Tokyo **10**, 6 and 12.

By Tadanori ONDOH

Geophysical Institute, Kyoto University

and Syoichiro HASHIZUME

Radio-physics Institute, Fourth Division,
National Deffence Agency, Tokyo

Abstracts of the Papers Presented at the 27th Annual Meeting, Tokyo, May 16–18, 1960.

MISAKI M. (Meteorological Research Institute) **Studies on the Atmospheric Ion Spectrum (I) The Relation between Electrical Conductivity and Small Ion Spectrum** ——A newly designed ion chamber has been constructed for the investigations of the mobility spectrum of atmospheric ions. After the preliminary examinations on the air flow in the chamber with the aid of smoke streaks and puffs, the appropriate flow rate has been determined. The present measurements of ion spectra, using the method previously developed by the author, were limited in the mobility region between 2 and 0.2 cm^2/volt. sec. An example of the diurnal series of spectra obtained in fair weather is shown with the values of electrical conductivity measured successively. From the analysis of these experimental results, it was deduced that there is appreciable contribution of large ions to the conductivity, and that the apparent values of small ion concentration obtained by the small ion counter of the ordinary type are too great by the fact that the counter collects appreciable amounts of large ions in the polluted air such as of the large city. The apparent mean mobility of small ions, deduced from the observed values of conductivity and apparent small ion concentration, have a tendency to decrease with increase of conductivity as suggested by O'Donnell. Direct measurements of mobility spectrum, however, show that either actual mean mobility of small ions, or the position of the peak of spectrum in the region of small ions, does not shift with the variation of conductivity.

SHIMIZU T. (Fukui University) **Capture of Ions by Charged Wire Rings**——Investigations on capture of ions by charged wire rings in the air current were made through the measurement of the dissipation coefficient (a) of electricity. Generally the a increases with the increase of the velocity of air current, and in most cases it has a maximum within 10 m/sec. The forms of curves showing the relation between the a and the velocity of air current are able to be classified into three types A, B and C on the whole. In consequence of the considerations it is proved that these three types are characterized by a certain constant σ introduced in the equation, by which the a and the velocity of the air current are connected. Observations were performed also in the air current containing smoke, in which the a becomes extremely small. Characters of the ratio (q) of the two dissipation coefficients of the negative and positive charge were pursued in detail, too. The q becomes small with the velocity of the air current and approaches to 1. It is closely related with the air temperature, humidity and pressure. The product of the a and humidity is related with the square root of the product of temperature and pressure. Relation between the q and the velocity of the air current is mainly dependent on the constant σ as well as the a.

KAMADA T. (The Research Institute of Atmospherics, Nagoya University) **On the Continuous Intensity Spectrum of Atmospherics from 2 kc/s to 100 kc/s (I) The Apparatus used**——As a work runs through the research of the intensity of atmospherics in VLF range, author produces the direct spectrum vision apparatus by way of experiment. This spectrum-analyzer uses the same continuous frequency scanning type as an SONA-GRAPH, which analyses atmospherics received within a setting hours as a function of both amplitude and frequency on one cut of 16 mm film. The antenna is a vertical rod with a height of 10 meters. The bandwidth of IF amp. is ± 500 c/s. Time variation of amplitude spectrums are indicated by the projection of this film. The purpose of this investigation is both the research of VIF ionospheric propagation and of the spectrum of atmospherics in VLF range. At present, a trial observation is carried out and a sudden shift of amplitude maximum region in spectrum is observed at the time of SEA, 5 April, 1960. Hence, it becomes clear that the continuous observation is important to the work of VIF ionospheric propagation.

OUTSU J. and IWAI A. (The Research Institute of Atmospherics, Nagoya University) **On the Electron Density Distributions in the Lower Part of the Outer Atmosphere**

Deduced from Whistler Dispersions——The evening and night-time values of electron density distribution in a height range 300 km to 3,200 km above the earth have been estimated from whistler dispersions averaged between 1605 and 1835 J.S.T. and 2205 and 0335 J.S.T., following the successive approximation method given by Allcock. The data used were obtained from observations at Toyokawa and Wakkanai stations during a period from July 1957 to Dec. 1959. In the calculation it is assumed that a ray path of a whistler is exactly along a line of force arising from a dipole at the center of the earth and the regular ionosphere exists between 100 km and 300 km and forms a parabolic distribution of electron density peaked at 300 km. The value of N_mF_2 used for the evening and night-time cases have been determined from the monthly median f_0F_2 at 1800 and 0400 J.S.T., respectively, observed at Kokubunji and averaged over the same observation period. The results are shown with solid curves in Fig. 1 and for comparison Allcock's distribution (broken line) $N=5.75\times10^4\exp(-h/2640)\,\mathrm{cm}^{-3}$ for 1,000–13,000 km and Maeda-Kimura's distribution (chain-like line $N_1=1.24\times10^6\exp\{-3.45\times10^{-3}(h-300)\}\,\mathrm{cm}^{-3}$ for $300\leqslant h\leqslant1{,}000$ km and $|\theta|\leqslant35°$, $N_2=1.8\times10^5\exp\{-6.57\times10^{-4}(h-300)\}\,\mathrm{cm}^{-3}$ for $1{,}000\leqslant h\leqslant16{,}500$ km or $|\theta|>35°$, are also shown in the figure. The distributions obtained almost lie between the Allcock's and Maeda-Kimura's distributions and do not decrease exponentially with the height as they do, but the rate of diminution appears too small in the region higher than about 2,500 km. The evening value is seen to be greater than the night-time one over the height range considered here. This seems to mean that the electron density diminishes during night at least up to the height of 3,200 km, though with a rate of decreasing degree. However, it must be noted that the results obtained depend on the assumptions about the form, height and value of density distribution of the regular ionosphere and the shape of the whistler ray path.

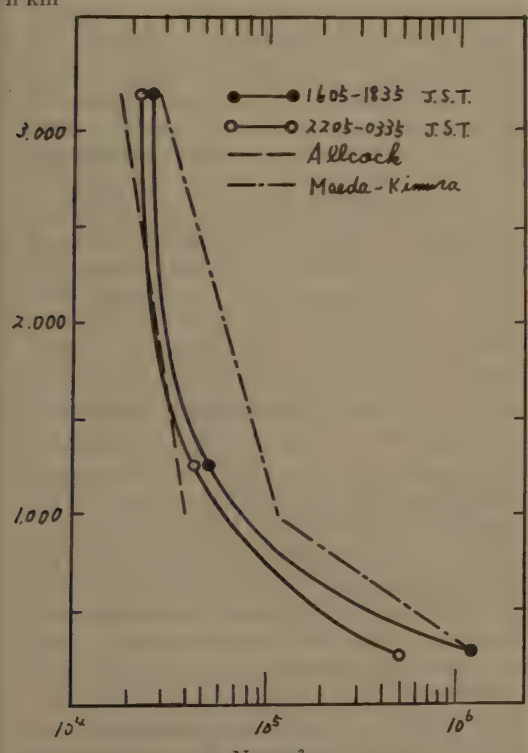

Fig. 1. Electron density 300–3,200km above the earth.

KIMPARA A. (Nagoya University) **On Some Remarkable Characteristics on Whistler Atmospherics**——The author describes some remarkable characteristics of whistlers observed in IGY and IGC for 2 years at Toyokawa and at Wakkanai in Japan. He found that the frequency of occurrence of whistlers has a definite seasonal variation due to thunderstorm activities and distributions of electron density and geomagnetic intensity in the exosphere. Correlation of the number of whistlers with geomagnetic activities, superimposed on this variation, is found very close in the period of heavy geomagnetic disturbances or of abundant occurrences of whistlers: Correlation coefficient of the effective K-index and number of whistlers on the 2nd day after geomagnetic disturbances is +0.60. The average dispersion of whistlers per month lags 2 months behind from solar activities expressed by sunspot numbers. Characteristics of dispersion of whistlers observed simultaneously at both stations are discussed in some detail. Diurnal and seasonal variations for 2 years are also described.

OGAWA T. (Geophysical Institute, Kyoto University) **Types of the Diurnal Variation of Air-Earth Current**——The daily percentage variations of the air-earth current were calculated every longitude of 90° over the world, using the percentage variation of the potential of the upper conducting layer (atmospheric total potential) deduced from *Carnegie* measurements over the oceans, and that of the columnar resistance obtained from the measurements by Sagalyn and Faucher. The

results generally represent the world-wide distribution of the measured daily variation curves which were arranged by Israël. This fact generally indicates that the daily percentage variations of the columnar resistance at the most stations over the land area are roughly equal, and also of the same magnitude as the universal daily percentage variation of the atmospheric total potential. However, more detailed discussions by comparing the measured and the calculated results at the urban district of the meridian 135° E show that the daily variations of the air-earth current depend more on the local columnar resistance than the atmospheric total potential, the percentage variation of the former being twice as much magnitude as that of the latter. It is suggested that at the urban district the nucleous concentration in the lowest layer of the exchange layer plays an important part in the atmospheric electric current system.

UCHIKAWA K. (Japan Meteorological Agency) **On the Atmospheric Electric Phenomena in the Upper Air (Relations to the Jet Stream)** —— Measurements of electrical conductivity and potential gradient in the upper air using special radiosondes were carried out at four stations in Japan during IGY. Results of the measurements were investigated. It has been found that the vertical distributions of conductivity and potential gradient are different according to the intensity of the "Jet Stream" in the atmosphere. When the jet streams are strong, gradients of the conductivity along the south to north axes crossing jet cores are larger than the ones when the jet streams are weak. Calculated values of the conductivity, which can be obtained from the theoretical equation, are closer to the measured values in the weak jets than in the strong jets. The values of the potential gradient in the lower part of the strong jet core are smaller than the ones in the same part of the weak jet core. The cause of these phenomena is deemed to be through the upper air current, and then vertical currents of air were calculated from the variations of small ion density obtaining from the measured conductivity. The results of computations are following: During the intensity of the jet is increasing, downward motions predominate except the south and lower part of the jet core. During the intensity of the jet is decreasing, characteristic is inverse.

ISHIKAWA H. (Research Institute of Atmospherics, Nagoya University) **On the Structure of a Positive Discharge to Ground** —— In contrast to a negative discharge to ground, a positive discharge to ground appears so seldom that we have not been able to succeed to collect sufficient data to discuss the structure of it till to the present days. Recent investigation of about 440 rapid field changes due to nearby ground discharges recorded by the author, however, has given him a few but reliable data concerning the discharge. The investigation of these data has made it possible to postulate the structure of a positive discharge to ground as follows: (1) Generally a discharge to ground is started by a igniting discharge that takes place between a positive charge pocket lying at the base of a thundercloud and a lowermost part of a negatively charged column streaching vertically through the middle part of the thundercloud. The discharge will become negative when the charge at the positive pocket predominates the charge at the lowermost part of the negative-column, and it will become positive when the relation between the two charge quantities are reversed. (2) Because the mechanism of positive charge accumulation at the cloud-base is mainly depending on positive point-discharges at the earth's surface, the charge accumulated is always insufficient to produce multiple strokes, therefore, statistically speaking, a positive ground discharge is expected to have a positive polarity only at their first strokes, and all the strokes following to the first to have a negative polarity, which point has been confirmed by the investigation of the records of the discharge so far obtained. It has not been possible to find out any difference between negative and positive discharges except for the polarity of stepped leader and return stroke involved in the first stroke.

MAEDA K., TAKEYA Y., MATSUMOTO H. and OKUMOTO T. (Department of Electronics, Kyoto University) **Atmospheric Temperatures and Wind Velocities by the Kappa-VI Rocket in the IGY** —— Atmospheric temperature and wind velocity in the region between the level readily attainable by radiosonde and the height of about 60 and 40 km have been obtained by our group with Kappa-VI rockets by means of rocket-grenade method. The two rockets were fired at 12^h03 on Dec. 23, 1958 and at 11^h45 on March 18, 1959, at Michikawa (39°34′ N, 140°03′ E) in Japan. The distributions of temperature and wind velocity of above two firings were calculated by our method in which the distributions are as-

sumed to take the form of quadratic equation with altitude. The results have nearly coincided with the data of Ft. Churchill in Canada. The result of Dec. 23 shows that there exists a small wind from west in the region of 25–50 km of height and a greater wind of about 100 m/sec from east in 50–60 km, and that of March 18 shows a wind of about 50m/sec from east in 20–40 km of height. The temperature of Dec. was similar to the summer pattern of Ft. Churchill and of March rather near to the winter pattern, but the mesopeaks had the highter values by about 5 or 10 degrees Kelvin than that of Ft. Churchill.

AKIMOTO S. and SYONO Y. (Geophysical Institute, Tokyo University) **Remanent Magnetization of Single Crystals of Ferromagentic Minerals**——Field dependence of thermo-remanent magnetization and isothermal remanent magnetization of single crystals of both natural magnetite, hematite and pyrrhotite and synthetic $YFeO_3$, was studied systematically. It was confirmed for all the samples that the character of thermo-remanent magnetization still exists in fairly large single crystals. The production of thermo-remanent magnetization is most effective in the parasitic ferromagnetic single crystals. Only several Oe of the applied magnetic field seems to be strong enough to saturate the thermo-remanent magnetization of hematite and $YFeC_3$ single crystals. The value of J_{TC}/J_S which may represent a degree of fixing of thermo-remanent magnetization is only 10^{-3} at most for the magnetite single crystal but even in this case the thermo-remanent magnetization is definitely distinguished from the isothermal remanent magnetization. Pyrrhotite shows an intermediate character between hematite and magnetite for the present study. Anisotropy of the remanent magnetization in various crystal axes is also examined for all the specimens.

UYEDA S. (Earthquake Research Institute, Tokyo University) FULLER M., BELSHE C. J. and GIRDLER R. (Department of Geodesy and Geophysics, Cambridge University) **Anisotropy of Magnetic Susceptibility of Rocks and Minerals**——There are two causes for the anisotropy in magnetic susceptibility of rocks and ferromagnetic minerals: 1) shape effect and 2) crystalline anisotropy. In general these two effects may act simultaneously but in rock-magnetism they are frequently separable. In the case of anisotropy due to the shape effect one can estimate the degree of anisotropy theoretically by ellipsoid-approximation, provided the magnitude of the bulk susceptibility is given. As for the general titanomagnetites (cubic), and the rocks containing them, anisotropy is chiefly due to the shape effect, whereas the crystalline anisotropy is dominant in the cases of the crystals of lower symmetry, such as ilmenite-hematite series and pyrrhotite. For magnetically anisotropic rocks and minerals, the direction of thermo-remanent magnetism was found to be deviated considerably from that of the external magnetic field. Several examples of interest and some theoretical considerations are given.

KOBAYASHI K. (Geophysical Institue, Tokyo University) **Chemical Remanent Magnetization VI**——It was concluded from the recent study that magnetization of the ferromagnetic precipitated particles in Cu–Co alloy behaves in such different manners as shown in the following lines at the three kinds of stages of particle growth induced by isothermal aging of the alloy. 1. (Initial stage of particle growth) Most particles are superparamagnetic, so that they are easily magnetized by a weak magnetic field but no remanent magnetization is formed. 2. (The second stage of particle growth) Particles change their magnetic behaviours from superparamagnetic to ferromagnetic according to the increase of the particle size. Under the influence of magnetic field magnetization of the alloy is frozen and memorized as a stable remanent magnetization like thermo-remanent magnetization. 3. (Final stage of particle growth) Remanent magnetization obtained in the second stage decreases gradually to a small amount as a result of the formation of magnetic domains. These results seem to be consistently and successfully extended to the interpretation of chemical remanent magnetization of rocks and ores. The author proposed the following grouping of chemically altered or weathered rocks, ores and chemical sediments according to the degree of particle growth. Group 1. (belonging to the second stage of particle growth)——remanent magnetization is strong and stable e.g. some ores and rocks bearing fine veinlet-like maghemite (previously reported), red sandstone occurring in Japan, England and other countries. Group 2.——weak and unstable remanent magnetization i) belonging to the 1st stage, e.g. Keuper Marl in England (Creer, 1957)

ii) belonging to the extreme case of the final stage, e.g. some titanomaghemite-bearing rocks in Japan, some kinds of metamorphic rocks Group 3.——weak but stable remanent magnetization (belonging to the medium case of the 3rd stage) e.g. artificially generated CRM, probably some kinds of metamorphic rocks and ores.

KOBAYASHI K. (Geophysical Institute, Tokyo University) and KUSHIRO I. (Geological Institute, Tokyo University) **Natural Remanent Magnetization of Dolerite Sheets** ——A study of natural remanent magnetization and other magnetic properties has been carried out for some Miocene dolerite sheets occuring at Atumi district (Kayaoka, Sumiyosizaki and Iragawa) in North-Eastern Japan. Results obtained so far are as follows; 1. Natural remanent magnetization of every specimen from dolerite sheets at Sumiyosizaki and Iragawa is weak and unstable. 2. In Kayaoka dolerite sheets, specimens from only one of localities where the rocks were formed in the early stage of crystallization of magma have stable and reverse (S12°W, 60°U) natural remanence, while the other are magnetically unstable and have much scattered polarization even in one block. The stability is also distinguished against demagnetization by alternating magnetic field. 3. Ferromagnetic minerals (titanomagnetite) from the dolerite sheets are generally oxidized, but remarkable characters of titanomaghemite (previously reported) can not be observed under the reflection microscope except one extremely oxidized specimen. 4. From the thermomagnetic measurements, thermally reversible and irreversible type of titanomagnetites are distinguished, but the difference is not necessarily correspondent to the other properties. 5. Andesite which was generated nearly in the same period as the dolerite sheets has a very stable natural remanent magnetization, direction of which is normal and well consistent with other results in Japan. Further investigations are now being continued, especially in relation to the origin of the reverse natural remanence.

DOMEN H. (Physical Institute, Faculty of Education, Yamaguchi University) **The Space Variation of the Natural Remanent Magnetism of Rocks**——The natural remanent magnetism (N.R.M.) and other magnetic properties of the rock specimens taken from the lava flows widely spreading in the northern part of Yamaguchi Prefecture, West Japan, were examined, and these results show that there is the "Space Variation" among the above-mentioned magnetic properties notwithstanding the fact that the lava flows from which these rock specimens were collected had been erupted simultaneously in the early Pleistocene; there are linear correlations between the logarithm of the intensity of N.R.M. and of the induced magnetization in the present geomagnetic field, and between that of the K—(=Jrn/Js) and Qn— ratio respectively. The relation between the advancement of the phase exsolution of the contained rock forming ferromagnetic minerals and the distribution of the direction of the N.R.M. was discussed. As a reason of such a space variation, the vertical distribution of the N.R.M. of the rock specimens taken from an outcrop of one lava flow, was discussed. When the N.R.M. of the rock specimen taken from the upper part of this outcrop was compared with that of the specimen from the lower part, roughly speaking, there is the linear correlation between the logarithms of the increments of the remanence and the depth from the surface of the lava flow. The same problems are also discussed on the sedimentary rock specimens taken from the tertiary layer in the Ube and the Susa Distruct of Yamaguchi Prefecture.

MOMOSE K. (Shinshu University) **The AC-demagnetization and the Measurement of Jn/Jtc of the Magnetism of the Pliocene Volcanic Rocks** —— Basing upon his geomagnetic researches for the Pliocene volcanic rocks in Central Japan, the author already pointed out that the pole position might have reversed continuously through the span of Pliocene times. Although some testifications in the examination of the stabilities of magnetism retained in these volcanic rocks are now in process, all these samples examined by AC-demagnetization assay have proved to be very stable as compared with the other known stable samples that have hitherto ascertained by various tests. Most values of Jn/Jtc of the samples, the pole position of which locate in low latitudes are indicated to be averagely 0.30, whereas those in which their pole positions locate in high latitudes are indicated to be comparatively larger (averagely 0.80). If the author is to appreciate the significance of the obtained results, he is inclined to suppose that the mo-

ment of geomagnetic dipole might have decreased through the process when geomagnetic field was reversing. There is, however, a little doubt in the belief that the properties of the contained magnetic minerals might not have transformed through the heating assay of obtaining T.R.M.

NORITOMI K. (Institute of Mining Geology, Mining College, Akita University) **The Electrical Conductivity in the Earth's Interior Estimated from That of Basic Rocks**——The electrical conductivity of olivine and basic rocks having olivine structure are related to the absolute temperature T by the equation

$$\sigma=\sigma_0 \exp\left(\frac{-E}{kT}\right) \qquad (1)$$

At high temperature and at ordinary pressure, the rocks show the three process of change in their conductivity. From the experimental data, the average values of σ_0 and E for each process are obtained as follows;

Table 1

σ_0 (Ohm^{-1} cm^{-1})	E(eV)	Temperature (°C)
1	1.4	600—1100
10	2.0	1100
10	0.8	1150

Supposing that the earth's mantle is composed of this type of ferromagnesian silicates, the conductivity within the mantle can be estimated by using the data of Table 1. In this case, the influence of pressure on the conductivity must be considered. Of the effects of pressure, the term of $\partial E/\partial P$ is the most important. According to the theory of ionic conduction,

$\partial E/\partial P=-E\chi\dfrac{\partial \log E}{\partial \log V}$ is obtained, in which χ is compressibility and $\partial\log E/\partial\log V$ is nearly -2 for all substances. If χ is related to the pressure by the relation $\chi=\chi_0 e^{-5\chi_0 P}$, the conductivity within the mantle is represented as a function of pressure:

$$\sigma_P=\sigma_S\exp\left[\frac{-E_0}{kT}\left\{\exp\left(\frac{2}{5}\right)\right\}\left\{\exp\left[\frac{-2}{5}\exp(-5\chi_0 P)\right]-\exp\left(\frac{-2}{5}\right)\right\}\right] \qquad (2)$$

In (2) we can substitute σ_S according to (1), putting E_0 equals to the values of Table 1, in order to obtain the relation between conductivity, temperature and pressure with the depth in the mantle. Substituting the temperature as given by Verhoogen (1956) and the pressure as given by Bullen (1940), the conductivity within the mantle is obtained as shown in the Figure.

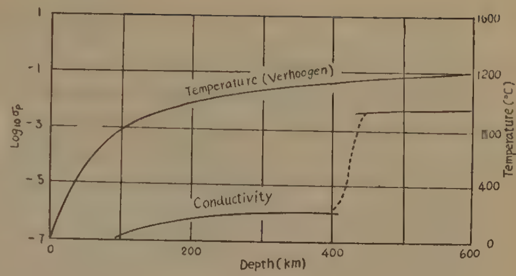

NAGATA T., AKIMOTO S., SHIMIZU Y., KOBAYASHI K., SYONO Y. (Geophysical Institute, Tokyo University) and KUNO H. (Geological Institute, Tokyo University) **Palaeomagnetic Study on Cretaceous Rocks in Kitakami District**——Palaeomagnetic study on Cretaceous rocks in Kitakami district of northeastern Japan has been continued as a sequence of the previous studies on Quaternary and Tertiary rocks in Japan. Rock samples were collected at five sites in three localities along the Pacific coast of Iwate and Miyagi prefecture. The results of palaeomagnetic study of the rocks of which magnetic stability was carefully examined are summarized in the following table (page 44). As seen in the table, the pole position of the lower Cretaceous is in the central Pacific ocean of the southern hemisphere, being nearly along the extension line of the polar path hitherto obtained from Tertiary and middle Cretaceous rocks in Japan.

KITAMURA M. and TEZUKA T. (Meteorological Research Institute) **On the Daily Variation of the Cosmic-Ray Intensity (I)**——In order to obtain the energy dependence of DS-component of cosmic-ray variations during the cosmic-ray storms, world wide data of cosmic-ray intensity during IGY were analysed for both mean diurnal variations of all days and storm time diurnal variations for all stations, respectively. The results of analysis are as follows: (1) The amplitude of diurnal variation of all days at about 50° in geomagnetic latitude shows the maximum value and those at equator and polar region are smaller than others. (2) On the contrary, the amplitude of semi-diurnal component of all days is maximum at equator, decreasing monotonically with latitude. (3) From these features of the latitude dependence mentioned above, it is infered that the diurnal component of time variation of cosmic-ray intensity is caused by the magnetically controlled mechanism, and the origin of the semidiurnal component consists in the earth's

locality	age	rock	Declination	Inclination	Pole position φ λ	error angle	number of samples	Intensity range
Ôhunato	lower Cretaceous	tuff	N58°W	3°	26°S 147°W	6°	20	$0.25\sim2.45\times10^{-5}$ e.m.u./gr.
Kesennuma	,,	basalt, red shale	S6°E	45°	22°S 150°E	10°	16	$1.82\sim217.4\times10^{-5}$
Ôsima I	,,	andesitic lava	N65°W	16°	24°S 139°W	6°	29	$1.36\sim109.9\times10^{-4}$
Ôsima IIa	,,	,,	N87°W	−13°	2°N 135°W	9°	15	$3.14\sim29.0\times10^{-5}$
Ôsima IIb	,,	black shale, tuff	N77°W	−2°	9°S 137°W	8	15	$1.00\sim7.98\times10^{-5}$

atmosphere. (4) The amplitude of the diurnal variation of the cosmic-ray intensity during the cosmic-ray storms shows the maximum value at 40°–50° in geomagnetic latitude, and diurnal component of DS for the integral intensity is nearly constant about 10 Bev. (5) The amplitude of the semi-diurnal variation of ccsmic-ray intensities during the cosmic-ray storms shows the maximum value at about 50°, and the semi-diurnal component of DS for the integral intensity is maximum at about 3 Bev. (6) For the event (4), we propose a model of expanding solar magnetic clouds in which the Forbush-decreases and DS are caused by the inverse-Fermi effect and the expanding velocity of the clouds outward from the sun is larger than that toward the sun. (7) Event (3) may be caused by the modal change of the atmospheric oscillation by the heating of the upper atomosphere in the auroral zone due to the auroral particles.

MURAKAMI K. (The Inst. Phys. Chem. Res.) **The Theoretical Investigation on the Diurnal Variation of Cosmic-Ray Intensity**——The world-wide distribution of the phase and amplitude of the diurnal variation in cosmic-ray intensity was theoretically estimated. The assumptions and conditions considered here are (1) The geomagnetic field is of centered dipole. Tilt of the axis is considered. (2) Anisotropy of the primary cosmic-ray flux is expressed by the sine wave distribution against the asymptotic geographic longitude. (3) Dependence of asymptotic amplitude against geografic latitude is of the cosine of latitude, and symmetric with equator. (4) Only vertically incident particles are considered. (5) Dependence with primary energy is assumed to be due to Fermi acceleration, electric field acceleration, and the combined type. Besides, Dorman's spectrum is also compared. (6) The yield function of neutrons are used so that the result can be compared with observations at sea level. The results of calculation showed that: the earliest phase is appeared at the equatorial region of South America, and the higher the latitude the later the phase. The world-wide distribution of phase and amplitude depends not only on geomagnetic but on geographic coordinate. The latitude dependence of the calculated result may indicate that the combined type is preferable to be compared with experimental data.

KUDO S. and MURAKAMI K. (The Inst. Phys. Chem. Res.) **The Diurnal Variation with Untiphase of Cosmic Radiation**——As was previously mentioned, the diurnal variation of the cosmic radiation observed on December 23, 1957, the amplitude of which was as large as 2% in the neutron intensity at high latitude, was markedly different from the ordinary diurnal variation on the following points; (1) The maximum time of diurnal variation on that day was about 3 o'clock in local time and was just untiphase to the ordinary variation. (2) As for the phenomena other than cosmic radiation, a flare in degree of Importance II was observed on the surface of the sun, but nevertheless the geomagnetism was quite calm. We paid attention to the diurnal variation with untiphase this time and tried to find out such variations as having more than 1% amplitude in neutron intensity at high latitude during the period from July 1957 to February 1959. The results of analysis show that: (1) flares occured on the surface of the sun on the day when the diurnal variation with untiphase was found, but it was not likely to be connected with the location of flare; (2) the decrease of cosmic radiation or the disturbance of geomagnetism was observed one or two days after the diurnal vari-

ation with untiphase was found; (3) the geomagnetism was comparatively calm when the diurnal variation with untiphase was observed. Secondly we investigated statistically the correlation between the solar-phenomena and the diurnal vatiation with untiphase, but we have not yet succeeded to obtain any significant result. To conclude the above investigation, it is probable that the diurnal variation with untiphase was caused by certain mechanism in the planetary space, by solar-phenomena or any other sources, and was observable on the earth when there happened to be no geophysical disturbances.

KANNO T. (Department of Physics, Fukushima University) **On the World-Wide Distribution of the Daily Variation of the Cosmic Ray Neutron Intensity and its Variation**——Data of the 39 stations in the world were employed during the period July –December, 1957, 42 stations during January –June, 1958, and 43 stations during July–December, 1958. These stations were classified into two groups; the one is the mountain height group ($\geqslant$2000 m above sea level), the other the sea level group ($<$2000 m above sea level). T_m, the local time of maximum intensity in the diurnal variation, was derived by the vector sum of the first and the second terms of the harmonics analysed on the monthly average diurnal variations. It seems that there is the latitude effect in T_m, which has the minimum value around the geomagnetic equator. The minimum values of the latitude effect curves in T_m have clear correlations with the sunspot numbers determined by the Zürich Astronomical Observatory in every months, and it appears that T_m advances as the solar activity becomes intense. From the lines of equal T_m in the world map, we can know that the world-wide distributions have the special tendencies having the minimum value of T_m in the region from the Pacific Ocean to the South Africa passing through the South America, and that these distributions tend to remove every month. From the results mentioned above, it may be suggested that the cosmic ray intensity is controlled with two factors—the one is due to the inner terrestrial magnetism, the other due to the modulations with magnetic clouds in the interplanetary space. It may be suggested that, from the former, there is the latitude effect on the average, and, from the latter, T_m advances as the solar activity becomes intense and the time variation of the world-wide distribution of T_m is resulted.

KODAMA M. (The Institute of Physical and Chemical Research) **Cosmic-Ray Increase on July 17, 1959**——The cosmic-ray increase observed on July 17, 1959 has been studied by using neutron data from 25 stations. This increase has the two features different from the past five unusual increases. (1) Energy spectrum is not so steep. (2) Time delay of the maximum intensity time in cosmic-ray from the solar flare time is very long. These facts suggest that a part of solar cosmic-ray particles trapped in the magnetic cloud ejected from the sun escape from the cloud on the way to the earth.

TORIZUKA K. (Tokyo Gakugei University) and WADA M. (The Inst. Phys. Chem. Res.) **The Onset Time of the Decrease of Cosmic-Ray Intensity**——The meson intensity have been measured in Tokyo by means of high counting apparatus (10 m²) of the Institute for Nuclear Study. The large and abrupt decreases in cosmic-ray intensity were succeedingly observed on July 11, 15 and 17, 1959. The onset times of the decreases were compared with those obtained at M.I.T., U.S.A. by means of the high counting apparatus. It was found that the differences amounted to one hour. The tendency that the onset time observed at the morning station was earlier than that of the evening station. It may indicate the anisotropy of cosmic-ray flux at the time of the decrease. Further investigation on such phenomenon will provide the knowledge of the interplanetary space in disturbed state.

KODAMA M. and WADA M. (The Institute of Physical and Chemical Research) **Intensity Minimum in Cosmic-Ray Neutrons during the IGY**——The long term variation in cosmic ray neutron intensity observed during the IGY from July 1957 to December 1958 represents a significant latitude dependence of its phase. The month of minimum intensity in the lower latitude stations is earlier than that in the higher latitude ones. It is suggested that this phase difference has been caused from superposition of the true long term variation and the short term variation, or Forbush type decrease. Intensity minimum of the true long term variation is found in January 1958.

KITAMURA M. (Meteorological Research Institute) **On the Mechanism of Cosmic-**

Ray Storms——The modulation mechanisms of the cosmic-ray intensities have been investigated hitherto by many investigators. They are devided into two groups of theories. One is the geocentric model and the other is the heliocentric model. However, the observation of the cosmic-ray storm by Explorer VI provided the convincing evidence which shows that we may not deal with geocentric model for the cosmic-ray storms. And then, two fundamental mechanisms on the point of view of the heliocentric model of the cosmic-ray storms are discussed in this paper: they are (1) the effect of the diffusion of cosmic-ray particles into the magnetic clouds, and (2) inverse-Fermi effect of cosmic-ray particles due to expansion of the magnetic clouds. Comparison of the theoretical calculations with the observational fact of the energy dependence of the decrement of the cosmic-ray intensities during the cosmic-ray storms shows that the machanism (2) is essentially important for the cosmic-ray storms, while the acattering lengths of cosmic-ray particles in the magnetic clouds are rather smaller than Larmor's radii.

KITAMURA M. (Meteorological Research Institute) and KODAMA M. (The Institute of Physical and Chemical Research) **On the Time Variation of the Energy Spectrum of Cosmic-Ray Particles during the Forbush-Type Decrease (III)**——We have previously obtained a empirical formula of energy dependence of the decrement of the cosmic-ray intensity during the cosmic-ray storms. Starting from this formula, we calculate the modulation factor, $\eta(E)$, as a function of energy, for the Forbush-type decreases, defined as:

$$I_s(>E)=\int_{E_\lambda}^{\infty} m(E)\eta(E)j_0(E)dE$$

where $I_s(>E)$: integral intensity during the cosmic-ray storms, $j_0(E)$: primary spectrum of cosmic-rays for normal state, $m(E)$: specific yield function, E_λ: magnetic cutoff energy. Thus, $\eta(E)$ obtained from this analysis, compared with the theoretical consideration, shows that inverse-Fermi effect of cosmic-ray particles due to the expansion of the magnetic clouds is more essential for the Forbush decreases than the other effect such as diffusion of the cosmic-ray particles into the magnetic gas clouds.

SAKURAI K. (Geophysical Institute, Kyoto University) **Propagation Mechanism of the Low Energy Particles Produced from the Sun**——It has been made clear that the low energy particles with energies a few Mev—several 100 Mev are produced in connection with the solar flares and then they impinge upon the geomagnetic high latitude regions. From the examination of their orbits in view of the same method as the solar cosmic rays, the following results are obtained; namely, (1) the local time effect of their incidence to the earth, and (2) the seasonal variation on their incidence frequency are expected. Thus, we expect that the above mentioned effects will be present at the pre-SC polar cap blackouts, which are estimated as the direct incidence of the low energy particles from the sun. If the propagation of these particles is associated with the magnetic clouds, we can not expect the local time effect of their incidence. As the observation does not also show this effect, we can conclude that their propagation occurs as trapping within magnetic clouds. We may therefore estimate the properties of the magnetic clouds.

KAMIYA Y., UENO H., KATO S. and SAGISAKA S. (Nagoya University) **The Design of Cosmic-Ray Analysor with Solid Iron Magnet**——In order to determine the sign of charge and the momentum in high energy cosmic-ray particles, a cosmic-ray analysor with a solid iron magnet is designed. This solid iron is the form of the cylinder with 50 cm diameter and 200 cm length and has a hole with 20 cm diameter, as shown in Fig. 1. The coils magnetizing it are consisted of 600 turns of copper wire. The magnetic flux passing through this magnet is required about 1.8 weber m^{-2}. Trays of neon hodoscope a, b, c and d inform the trajectory of penetrating particle. The effective areas of outer trays (a, d) are 100 cm × 100 cm and inner trays (b, c) are 65 cm × 65 cm, respectively. In each tray, there are thin neon tubes (diameter 1 cm) and a half of them are set in cross each other. They are triggerd by the 2 fold coincidence of plastic scintillators (A, B) and side showers are excluded by the anti-coincidence of another tray. Using camera system with 16 mirrors, each event is recorded in a photograph. The maximum momentum of particle to be de-

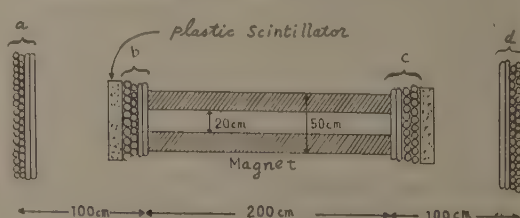

Fig. 1

tectable by this apparatus is estimated about 60 Bev.

Kondō I., Murayama T., Mori S., Mishima Y., Okuda H., Sakakibara S. and Makino T. (Physical Institute, Nagoya University) **On the Construction of Cosmic-Ray Telescope No. 3**——A new telescope for the observation of cosmic ray particles is now under construction at Nagoya Universtiy. This telescope (Cosmic Ray Telescope No. 3) uses only the Cerenkov radiation emitted by cosmic ray particles in air for detection of particles passage. Figure 1 shows

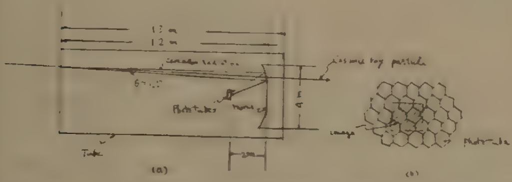

Fig. 1 (a) The geometry of the telescope.
(b) The image at the focus.

the geometry of the telescope. Cerenkov lights (400 photons/single particle) are reflected by parabolic mirror which are composed of 1172 small mirrors (each$\sim$100 cm^2). The shapes of the small mirrors are so designed to make the size of the image at the focus as 30×30 cm^2, and light distribute uniformly over 4$\sim$5 phototubes. In order to convert U.V. in the Cerenkov light into visible light, wave length shifter is coated on the surface of phototube, thus increases the light pulses almost to twice. The pulses from the phototubes are amplified ($x\sim10^4$, $t_r=100$ mμsec), and then selected for 4-fold coincidences ($\tau=100$ mμsec) among neighbouring phototubes, thus discriminating the signal pulses from noise. The output of the coincidence circuits are then mixed to make a certain resolution angle, and counted by scalers, then recorded by a recorder consisted of parametron units. By this arrangement, the direction of single high energy mu-meson ($>$4.3 Gev) can be detected with accuracy of $\pm2°$. The field of the telescope is about 10° (in zenith angle) and 20° (in azimuthal angle). Counting rate of each component will be about 6000 at zenith and 400 at $\zeta=80°$ per hour respectively.

Kamiya Y., Sagisaka S., Ueno H. and Murayama T. (Physical Institute, Nagoya University) **Observation of the Point Source of Cosmic Rays**——Observation of the point source of cosmic rays with two G-M counter telescopes was continued in 1959, in a similar way to that in 1955–1958. A part of the celestial sphere (right ascension: 23h–11h, declination: 10N–15S) was observed twice a day. On the data averaged through the year, no remarkable point source was found in the above mentioned field. Small differences among the intesities of each subdivided part are consistent with that they are only due to the statistical fluctuation. Special attention was paid to the region in Orion, which was recognized as a point source from the results of the observation during the period from April 1954 to December 1956. In 1959, however, no intensity increase was found in this region, compared with the mean intensity in the same declination band (−0.89 1.36). But it cannot be ruled out that this source showed higher intensity during the short period in the year. At the Moscow conference, correlation between the point source intensity and the luminosity of a variable star "W-Orionis" was suggested by one of the authors. This star showed significant increase of luminosity during the period from Nov. 15 to Dec. 27 1959 (about 0.7 m in magnitude), and remained nearly constant in the following two months. While the point source intensities were +11.7 5.0 and −5.5 3.0 in the two periods mentioned above, respectively. This fact suggests that the point source of cosmic rays is connected in more complicated way to the star than that considered before.

Tohmatsu T. and Kaneda E. (Geophysical Institute, Tokyo University) **Latitudinal Dependence of Nocturnal and Seasonal Variations of the Oxygen Green Line in the Night Airglow**——Nocturnal and seasonal variations of [OI] 5577 radiation are studied by using the observational data from 14 stations in low and middle latitudes during I.G.Y. and I.G.C.. The results obtained may be summarized as follows. 1. The variation of an individual night can be divided in two parts; one, the regular part which varies dependent on local time, latitude and season, and the other, the irregular part which varies sporadically from night to night. 2. The 5577 radiation has a definite form of seasonal variation which is characteristic with respect to the geographic latitude. In the lower latitudes, the variation is semi-annual having two maxima in April and October, and two minima in January and July. In the middle latitudes, however, the variation is almost of annual character having one large maximum in October and two small

maxima in February and June. By comparing the variations from the stations on both hemispheres, it is shown that the variation is not annual but seasonal. 3. No correlation with the geomagnetic activities has been found. 4. The latitude effect of the intensity and its seasonal variation are studied by using the latitudinal profiles obtained by the "Soya", the ship of Japanese Antarctic Research Expedition, 1956/58, after applying the seasonal correction anticipated from the seasonal variations from several fixed stations in various latitudes. 5. The observational results are tentatively interpreted in view of the dynamical structure and the subsequent dissociative state of oxygen in the O_2–O transition region in the upper atmosphere.

YONEZAWA T. (Radio Research Laboratories) **On the Electron and Ion Density Distributions in the *F* Rgion**——The mechanism of formation of the *F* layers has been considered and theoretical electron and ion density distributions from the lower *Fl* region up to a height of 800 km or so above ground have been obtained. As the representatives of solar radiation the Lyman continuum and the resonance lines of neutral and ionized helium at 584 and 304Å have been taken into account. As regards the mechanism of removal of O^+-ions, the author has assumed ion-atom interchange reactions between O^+-ions and N_2- or O_2-molecules followed by dissociative recombination between the resulting molecular ions and electrons. Other molecular ions such as N_2^+'s are also assumed to disappear by dissociative recombination. Except in the lower part of the *F* region the effect of electron-ion diffusion in the gravitational field has also been taken into consideration. The calculated electron and ion density distributions have been compared with those obtained by rocket or satellite observation as well as by the technique to obtain an electron density *vs* true height profile from ionograms. In the lower *F* region the agreement between theory and observation seems to be satisfactory in the cases of electron density, in the case of ion density, however, the calculated number density of O^+'s is considerably lower, and that of O^+_2's considerably higher, than the corresponding observed values though the calculated number density of NO^+-ions seems to be adequate. There is also a difficulty concerning the values to be taken for the rate coefficients of ion-atom interchange reactions, i.e. these values must be taken to be smaller by one or two orders of magnitude than laboratory values of similar reactions in order to bring about as close an agreement as possible between theory and observation. Above the level of maximum ionization of the F_2 layer, on the other hand, a close agreement has been obtained between the calculated and observed electron density distributions at least up to a height of about 130 km or so above the level of maximum ionization, if a scale-height gradient of 0.3 is assumed, but the calculated and observed curves deviate more and more widely from each other at higher and higher levels, and the calculated value reaches only about a half of the observed one at a level 450 km above the level of maximum electron density.

SHIMAZAKI T. (Radio Research Laboratories) **The Occurrence of the Spread-*F* and the Geomagnetic Field** —— In the previous study, the writer clarified that most of the statistical properties of the occurrence probability of spread-F—such as daily, latitudinal and seasonal variations—much differ at higher and lower latitudes. It was also found that the correlation between the occurrence probability of spread-F and the *geomagnetic activity* is strongly positive at latitudes higher than 20° in geomagnetic latitudes, while strongly negative at lower latitudes. These are further confirmed most generally in the present report. This may enable us to believe that the entry of charged particles into the upper atmosphere is the primary cause of producing the spread-F at higher latitudes. A detailed study on the world's morphology of the occurrence probability of spread-F in some severe magnetic storms gives another evidence that strongly supports this consideration. In the present study, the effect of the geomagnetic storm is also investigated in full detail. After classifying the storms during Jan. 1957 to Sept. 1959 according to their intensity, the time (in U.T.) and the season of Sc, the occurrence probability of spread-F is compared with each other of various days before and after Sc for each group of the classification. The result shows that the occurrence probability of spread-F increases appreciably on days after Sc at higher latitudes, while decreases at lower latitudes. This tendency of the storm effect is most remarkable in storms of highest class of intensity and in those occurred in equinoctial seasons. The possible difference of the effect among various storms occurred at different times (in U.T.) is not so clearly confirmed from

the present study. This is probably due to the poor number of the storms during the period of the present study and the non-uniform distribution of those Sc's in time of the day. The spread-F at lower latitudes seems to originate from the instability of the earth's upper atmosphere itself. It is shown that the correlation of the occurrence probability of spread-F and the *magnitude* of the geomagnetic field is strongly positive at lower latitudes. At first sight, this is quite strange, because it may rather be supposed that the magnetic field tends to prohibit the turbulent motions from developing in the magnetohydrodynamic medium (ionosphere). We can see, however, the experimental result indicating that if the turbulence is produced from the laminar flow, the applied field tends to destabilize the flow resulting in the development of the turbulence. It is evident that considerable wind flows in the upper atmosphere, particularly strongly in the equatorial regions. Thus, the result can be understood at least qualitatively, but there still remains the problem unsolved quantitatively.

HAKURA Y. (Hiraiso Radio Wave Observatory, Radio Research Laboratories) **Statistical Patterns of Polar Cap Blackout and Auroral Zone Blackout**——It was already shown by the present authors that there are two characteristic types of polar blackouts (enhanced ionizations of polar ionosphere). One is polar cap blackout which appears with some hours delay after a major solar radio outburst of type IV. The other is auroral zone blackout which develops after the onest of geomagnetic storm. By the statistical analysis of 10 typical disturbances during IGY, characteristic patterns of both polar cap and auroral zone blackouts were obtained. Statistical pattern of polar cap blackout is confined within the geomagnetic latitude of about 60°~65°, and is characterized by a remarkable diurnal variation, being much intense by day than by night. On the other hand, the region of auroral zone blackout elongates towards lower latitudes in the morning hemisphere, though it ti superposed with the polar cap blackout, lasting even after the onset of geomagnetic storms.

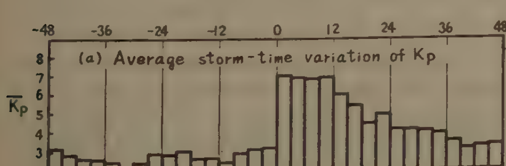

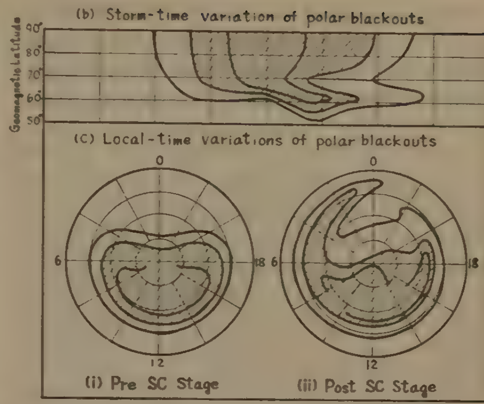

Fig. 1. Statistical patterns of the polar blackouts;
(a) Avarage storm-time variation of K_p,
(b) Storm-time variation of percentage-occurrence frequency of polar blackouts with respect to geomagnetic latitude,
(c) Local time variations of percentage occurrence of polar blackouts (Contour lines are drawn in 20% step, and hatched regions are greater than 60%).

MIYA K., SASAKI T. and ISHIKAWA M. (Kokusai Denshin Denwa Co., Japan) **Observation of F-Layer and Sporadic E Scatters at VHF in the Far East**——Properties of sporadic E scatter and F-layer scatter have been investigated by two transmission tests canducted over the Okinawa-to-Tokyo path (1480 km) and the Philippines-to-Tokyo path (2580 km) operating at frequencies of about 50 Mc/s. Sporadic E scatter is often observed on Okinawa signal in the evening hours by a gradual increase of signal strength about 30 db in the maximum above the normal level of the E-layer scatter. It has the closest correlation (0.94 in correlation ratio) with the occurrence of sporadic E affixed by the descriptive symbol "M" of all ionospheric factors. Bearing of the Es scatter shows a regular diurnal variation similar to that of the normal E-layer scatter. F-layer scatter generally appears on philippine signal in autumn when F-layer at the path midpoint displays an anomaly denoted by the symbol "R" or "S" having a top frequency of higher than 14 Mc/s. A pulse test exhibited a pattern of multipath signals extending over more than one millisecond. Bearing of the F-layer scatter gradually deviates westwards from the great-circle path with the lapse of time late in the evening.

KANAYA S. and YOKOI H. (Kokusai Denshin Denwa Co., Ltd., Tokyo) **The Lateral**

Deviations of the Radio Wave from Europe ——The measurements of bearings of BBC signals were made every season, and the following phenomena of lateral deviations were found out. (1) Southward deviation: When the MUF of the great circle path decreases below the used frequency, the bearings, in general, deviate southward. From minute observation of the deviation during the transient period, as seen in the figure, it may be seen that the bearings become stable in south-south-west direction after deviation due south or unstable wide variation. Such a transient lateral deviation may be explained thereby that the transition of the nondeviative and deviative absorption shifts the propagation path of the comparatively intensive signal scattered on the vast area includings many islands in South-East Asia and Australia. (2) Northward deviation: It was observed mainly on 15 Mc/s band that the radio wave arrived on the bearing northward by 10° to 30° from the true bearing. The northward deviation in daytime is regular at all seasons but it is not the case at night. The daytime deviation may be explained by ground forward scattering on Siberia. At night, however, althought the wave of Mc/s band arrives on the true bearing, as seen in the figure, the wave of 15Mc/s band deviates northward. This cannot be explained by the ground scatter and seems to be one of the special phenomena observed on the propagation path passing the vicinity of the auroral zone.

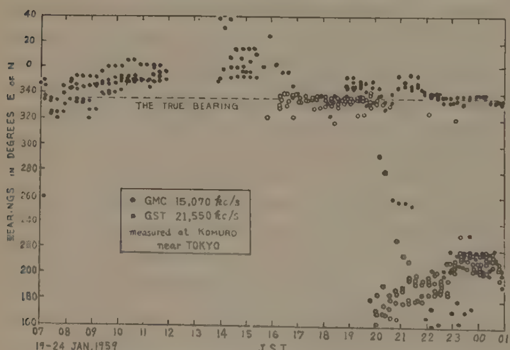

Fig. 1. The measured result of the bearings on 15 Mc/s and 21 Mc/s bands of BBC at Komuro Receiving Station, January 19–24, 1959.

RIKITAKE T. and TANAOKA I. (Earthquake Research Institute, Tokyo University) **A Differential Proton Magnetometer**——A magnetometer that records differences in total geomagnetic intensity between two points is described. By mixing the signals caused by free precession of protons from the two detecting colis, the beat signal is recorded on a pen-writing oscillograph. According to the test of the apparatus at the Oshima Geophysical Observatory, the accuracy of the differential magnetometer is found to be about 0.2/10 m at the moment. Since it is easy to increase the distance between the two coils, the sensibility of the apparatus can be increased. The purpose of the present apparatus is to detect very accurately local anomalous changes in the earth's magnetic field which might be accompanied by activities of Volcano Mihara.

YUKUTAKE T. (Earthquake Research Institute, Tokyo University) **Non-Steady State of Self-Exciting Dynamos II**——Time dependent behaviours of two conducting spheres rotating in an infinitely extended conductor as in Fig. 1 are studied. Induction equations are approximated by those expanded up to the second time derivatives of the mag-

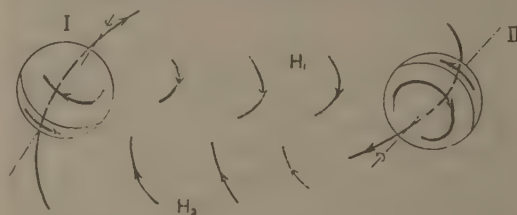

Fig. 1. A system of self-exciting dynamo.

netic field. Results of numerical integrations are classified into the following two: 1) The speeds of rotation of the spheres decrease endlessly while the magnetic field increases indefinitely. It is incomprehensible, from the physical point of view, that these states continues without limit. The difficulty might still be caused by the crudeness of approximation, though the second order terms of induction equations are taken into consideration. 2) The magnetic field decreases with the increase in the angular velocities. The spheres are accelerated by the external forces that have nothing to do with the generation of magnetic field while the magnetic field dissipates its energy as Joule heat. In some special cases, which belong to class 2), the magnetic field changes its polarity with diminishing amplitudes. The periods of the damping oscillation are about 1.3×10^4 years when the spheres of 500 km in radius are supposed to be rotating about 1100 km apart from each other in the earth's core. If the work done by the external torque is assumed

to be 10^{-16} erg/sec cm^3 which seems far short of the generally presumed thermal energy 1.7×10^{-7} erg/sec cm^3, the order of magnitude estimate shows that the magnetic field and the surface velocity of the sphere become 10^{-3} gauss and 5×10^{-2} cm/sec respectively. If the energy of the order of 10^{-7} reg/sec cm^3 is assumed, the above considered process does not seem always hopeless of affording the production of the enough field responsible for the secular variation of the earth's magnetic field.

NAMIKAWA T. (Institute of Polytechnics, Osaka City University) **The Occurrence of Overstability of a Layer of Fluid Heated Below and Subject to the Simultaneous Action of a Magnetic Field and Rotation** —The instability of a horizontal layer of fluid heated below, subject to an effective gravity $\boldsymbol{g}$, a magnetic field $\boldsymbol{H}$ and the Coriolis acceleration resulting from a rotation $\boldsymbol{\Omega}$, acting in the direction of the vertical, was examined by Chandrasekhar (1954, Proc. Roy. Soc. A, 225, 173; 1956. ibid. 237, 476). But the condition for the occurrence of overstability was not discussed. In this paper, the principle of the exchange of stabilities is examined for the case of both bounding surface free and it is shown that it is valid if $\kappa<\nu$, $1/4\pi\mu\sigma$ where κ, ν, μ and σ is the coefficient of thermometric conductivity, kinematic viscosity, magnetic permeability and electrical conductivity respectively; but when $\kappa>\nu$ or $\kappa>1/4\pi\mu\sigma$, it is shown that instability can arise either as cellular convection or as overstability (*i.e.* by oscillation of increasing amplitude) depending on the magnitude of $\boldsymbol{H}$ and $\boldsymbol{\Omega}$.

RIKITAKE T. (Earthquake Research Institute, Tokyo University) **The Effect of Ocean on Rapid Geomagnetic Changes** —— With the aid of two-dimensional experiments and mathematical theory, the electromagnetic induction in a conductor covered by a conducting sheet is studied. Applying the results to the effect of ocean on rapid geomagnetic changes, it turns out that the previous estimate of the ocean effect based on the induction in a single sheet is an overestimate. C. S. Cox's model, by which he explained the anomaly of geomagnetic variation in Japan as the effect of ocean at its margin, is also criticized. The writer is of the opinion, contrary to Cox, that the anomaly is likely to be caused by the induced electric currents at some depth in the earth's interior beneath Japan.

YOKOYAMA I. (Geophysical Institute, Hokkaido University) **Relation between Geomagnetic Variations and Telluric Current Variations**——One of the Maxwell's equations

$$-\frac{\partial(\varDelta Z)}{\partial t}=\frac{\partial(\varDelta E_y)}{\partial x}-\frac{\partial(\varDelta E_x)}{\partial y}$$

was already experimentally verified for the actual observations of earth-current by A.P. Bnodarenko (Dokl. Akad. Nauk, SSSR, **89** (1953), 443–445) although he analyzed the variation of which period was about 11 hours. From this relation, $\varDelta Z$ proves to depend on anisotropy of electrical conductivity of the earth. Assuming the horizontal layer-structure as the first approximation, one can determine the principal axes of the above anisotropy by means of the observations of $\varDelta Z$ and $\varDelta E$. Then, this direction coincides with the predominant one of the earth-current variations. The data obtained at Dourbes, Belgium were analyzed from this standpoint and the local anisotropy of conductivity was ascertained there. The anomalous behaviour of geomagnetic variations of short period in Japan and Germany may be connected with the local anisotropy of electrical conductivity of the earth.

NAGATA T. (Geophysical Institute, Tokyo University) **Geomagnetic Secular Variation in the Southern Hemisphere, Especially in Vicinity of the Antarctic** —— In the past several years, including IGY and IGC 1959 periods, a fairly extensive geomagnetic measurements were carried out in the Antarctic region. From results of these measurements, annual rates of geomagnetic secular variation are available at 12 points, among which 9 are on the Antarctic continent and 3 are on islands in the South polar region. Analyzing distribution characteristics of these data together with the similar data in the other parts of the earth, it is found that geomagnetic secular variation is anomalously large and complicated over and around the Antarctic. Its annual rate takes maximum near the Syowa station (69°00′S, 35°35′E), Z being 181 γ/year. Generally speaking, centre of vortices of the subterranean current system equivalent to the secular variation are situated near Syowa ($Z\simeq200\,\gamma/y$), near Heard Island (53°02′S, 73°22′E, $Z\simeq-100\,\gamma/y$), and near Marine Byrd Land (60°S, 100°W, $Z\simeq150\,\gamma/y$) in the concerned region. Excluding these three centres, there are only two remarkable centres over the earth, namely, near North-East coast of South America ($Z\simeq-100\,\gamma/y$), and near

Caspian Sea ($Z \simeq -60\gamma/y$). It may be said therefore that geomagnetic secular variation is much more active in the Southern hemisphere, especially around the South pole, than in the Northern hemisphere.

YANAGIHARA K. (Magnetic Observatory, Kakioka) **Characterization and Classification of Geomagnetic Pulsations (Second report)**
Characterization and classification of geomagnetic pulsations have been already reported by the present author. In this report, they are compared with the recent results reported by the other researchers, mainly by the USSR scientist. V. Troitskaya has discussed classification of pulsations in her article, continuous pulsation (pc) and pulsation trains (pt) in the Arctic and in the Antarctic (Symposium at Utrecht). Greater parts of her characterization and classification are consistent with our results on pulsations in middle or low latitudes. But her pc°, a subgroup of pc, is considered to be corresponding to our irregular but pt-like pulsations. For classification of general pulsations, characters appearing in typical pc or pt are better criteria. But it is not suitable in this case to consider that characters of "continuous" for pc, or "trains" for pt, only are the typical and representative characters. For example, period of oscillation is an important character. After the reexamination, it is concluded that any substantial modification is not necessary for the classification previously reported by the present author.

KURUSU K. and YANAGIHARA K. (Magnetic Observatory, Kakioka) **The Horizontal Disturbing Vector of Geomagnetic Micro-Pulsations, pc** —— The daily behaviour of the horizontal disturbing vector of pc-type pulsations has been studied using the induction magnetograms obtained during the IGY at Memambetsu ($\varphi=43°55'$N, $\lambda=144°12'$E) and Kanoya ($\varphi=31°25'$N, $\lambda=130°53'$E). The principal results are summarized as follows. (1) The most part (80%) of the azimuth of disturbing vector lies in the N-W quadrant at the two stations. The maximum number of appearance of the N-W azimuth falls on about 9h LMT. (2) The most part (80%) of the ratio (b/a) of the length of minor axis to major one of the ellipse described by the end point of disturbing vector are less than 0.5 at the two stations. Comparing the ratio b/a with the azimuth α during the daytime at Memambetsu, b/a has the least value, about 0.2, when the azimuth is directed most westerly, about N-W direction, before noon, whereas b/a reaches the largest value, about 0.5, when α is near the N direction after noon. (3) The most of all the disturbing vector rotates counterclockwisely. The maximum number of appearance of the counterclockwise rotation falls on about 15h LMT, whereas the clockwise rotation appears most frequently at about 08h LMT, at Memambetsu. (4) Comparing the present analysis of the distribution of azimuthal angle and rotational sense of pc in the daytime with the Terada's (1917) and Hatakeyama's (1938) results on pulsations not distinguished pc from pt or others close similarities on them are found in the daytime behaviour.

UTASHIRO S. (Hydrographic Office, Maritime Safety Board.) **On the Local Character of the Geomagnetic Pulsation, Pc**—— The local character of Pc observed by induction magnetograph at the Japanese four observatories (Memanbetsu, Onagawa, Simosato and Kanoya) was studied in the previous paper, and it was found that period or mode of local Pc at the four stations in Japan changes with latitude, and local Pc occurrs more frequently in the higher latitude than in the lower latitude. Now, if it is assumed that such characteristic phenomena caused by means of the hydromagnetic oscillations in the region between the inner Van Allen Belt and ionosphere, two mode of oscillation exist in this region, one is the toroidal and the other is the poloidal oscillation. The toroidal wave is propagated along the magnetic line of force and the poloidal wave at right angle to it. The sum of the poloidal and toroidal oscillations can be observed at the four observatories as local Pc pulsation. The period of the poloidal oscillation in the region between the inner Van Allen Belt and ionosphere can be calculated as follows:

$$T_p=\int_{r_0}^{r}\frac{2dr}{V}$$

where, V: velocity of Alfven wave, r_0: height of ionosphere at equator, r: height of inner Van Allen Belt at equator. The velocity $H/\sqrt{4\pi\rho_i}$ varies very rapidly against the height from the ionosphere to inner Van Allen Belt. Desseler calculated the velocity distribution with altitude. Using Desseler's results, the period of the poloidal oscillation calculated in this region becomes about 20^s at four stations. On the other hand, with respect to the toroidal oscillation:

$$T_t = \int_{\theta_0} \frac{2dS}{V}$$

where θ_0: co-latitude. The values of period calculated by means of the same method at each stations is as follows, Memanbetsu —— $T=47^S$ Onagawa —— $T=42^S$. If it is assumed that the magnetic hydrodynamic wave is produced by means of a corpuscular stream from the sun at the outer surface of the inner Van Allen Belt, as a magnetic line of force through Simosato and Kanoya does not reach to the inner Van Allen Belt, the toroidal oscillation is unable to be observed at these stations. Therefore, the poloidal and toroidal oscillations are observed in the higher latitude, and only the poloidal oscillation is observed in the lower latitude in Japan, that is, local Pc occurrs frequently in the higher latitude than in the lower latitude.

SAITO T., WATANABE T. and TAMAO T. (Geophysical Institute, Faculty of Science, Tôhoku University, Sendai) **On the Latitudinal and Longitudinal Effects of Geomagnetic Pulsations**——Analysing the magnetograms observed at the 5 observatories (PB, BD, Si, Fr, and Tu.) and auxiliary, Onagawa, Japan, the following characters of geomagnetic pulsations are obtained. (1) Pulsation in the period range 1 to 2 minutes. i) The range of this pulsation is larger in the higher latitude. ii) Generally, period of oscillation becomes to short from night time to daytime. iii) It seems that the amplitude variation does not depend so on L.T., but on U.T.. (2) pc type pulsation. (A) Latitudinal and longitudinal effects. i) Amplitude is larger at the northern observatory than at the southern one. ii) Maximum time of diurnal amplitude variation at Fr. is observed in the afternoon, while it tends gradually towards the morning at the northern or western observatories. (B) Seasonal variation. Diurnal occurrence probability curves of pc observed at Onagawa have maximum at 7～8 L.T. in winter, while it swells up towards the noon in summer. (C) Discussion i) Refering to the short research of pt previously analized by the authors, it seems likely that pc is excited in higher latitudes than pt. ii) It is supposed that the precession of the earth's dipole axis around the rotational axis makes the creeping of diurnal maximum time of pc according to the variations of the latitude, longitude and season.

SATO T. (1st Research and Development Center, Japan Defence Agency) **A Giant Pulsation during the Geomagnetic Storm of February 11, 1958**——A giant pulsation was recorded at all stations over the world at the same time as that of ssc of geomagnetic storm which occurred at 1^h26^m (UT) on February 11th 1958. The giant pulsasation continued during several hours and was accompanied by the severe auroral display, and by the large variations of earth current, micropulsation vector with short period, intensitites of consmic ray, cosmic noise and critical frequency of the ionospheric F_2 region. The anlysis of the pulsation using the magnetogram at 42 stations of the world shows the following characteristics. (1) The periods of the pulsation are almost equal at all stations of the world at any universal time. The period is not constant during the pulsation, but varies with the progress of the storm between 1.5 and 3.5 minutes. (2) The variations of the horizontal component (H) are in phase over the world, but the phases in the declination (D) and vertical component (Z) are respectively inconsistent with each other. In northern hemisphere the D component varies eastwards in the forenoon and westwards in the afternoon, while, the Z seems to vary somewhat irregularly. (3) The amplitudes of the variations for three components in the forenoon stations (especially early morning) are greater than in the afternoon and greater in the auroral zone than the lower latitudes. Maximum amplitudes recorded are above 400^γ in H, $30'$ D and 200^γ in Z. The direction of variation of magnetic vector and the characteristic of local time dependency of the variation amplitude resemble respectively the corresponding ones of the usual giant pulsation in the auroral and subauroral zones which occurs mainly on the disturbed day in progress of the bay and after the bay and has the maximum amplitude during the hours centered at 8^hLT. This fact implies that the giant pulsation of Feb. 11 is probably caused by the same origin as that of the usual giant pulsation. In other words, the latter is a world-widely simultaneous phenomenon which appears in middle and low latitudes only during morning hours on greatly disturbed day. The simultaneous pulsation over the world such as that of Feb. 11 appeared in other great storms, for example, on Sep. 4th, 13th, and 22th 1957.

YAMAGUCHI Y. (Kakioka Magnetic Observatory) **S.I. (Geomagnetic Sudden Impulse) and Pulsation**——At many magnetic observatories in Western Europe, a remarkable giant pulsation was observed on 17 July 1958. The giant pulsation started at 09

15 hours and ended at 12 45 hours at Witteveen. At other stations, the phenomenon started at nearly same time. On the day, continuously lasting pulsations (p.c) with periods of about 12 seconds and amplitudes of a few gammas were recorded and disappeared at 09 30 hours with a sudden impulse and the giant pulsation began. Does sudden impulse effect the pulsation of the geomagnetic field? This author examined whether the amplitude and the period of the pulsation show the difference before and after the occurrence of s.i., statistically. The results are abstracted as follows; 1) s.i. may not affect on the amplitude of pulsation ii) s.i. may not affect on the period of pulsation iii) s.i. (-c) may have some relation with the ending of pc.

OBAYASHI T. (Hiraiso Radio Observatory, Radio Research Laboratories) **Propagation of Solar Cosmic Rays Through Interplanetary Magnetic Field**——In recent years evidence has been accumlating that low-energy solar cosmic-ray particles arrive at the earth following intense solar disturbances. The time-delay of polar cap absorptions and of geomagnetic storms, which followed after an intense solar radio outburst of type IV, indicates the fact that solar cosmic-ray particles originating to the west of the solar central meridian reach the earth earlier and more easily than those from the east. The model of the interplanetary magnetic field, which may be appropriate for the explanation of this evidence, is given as follows: The interplanetary magnetic field will be formed by the outward-streaming solar winds which carry the imbeded solar magnetic fields and the lines of force also being linked with the sun itself. The rotation of the sun produces a curvature of streams and consequently of the lines of force, which are convex towards the west: Since the injected solar particles will tend to travel along the existing magnetic lines of force, this model can give the explanation of the western excess of the arrival of solar cosmic rays as well as the inequality of their travel-time with respect to the heliographic position. It is shown that the estimated intensity of the magnetic field is found to be of the order of 10^{-4} to 10^{-5} gauss near the earth's orbit.

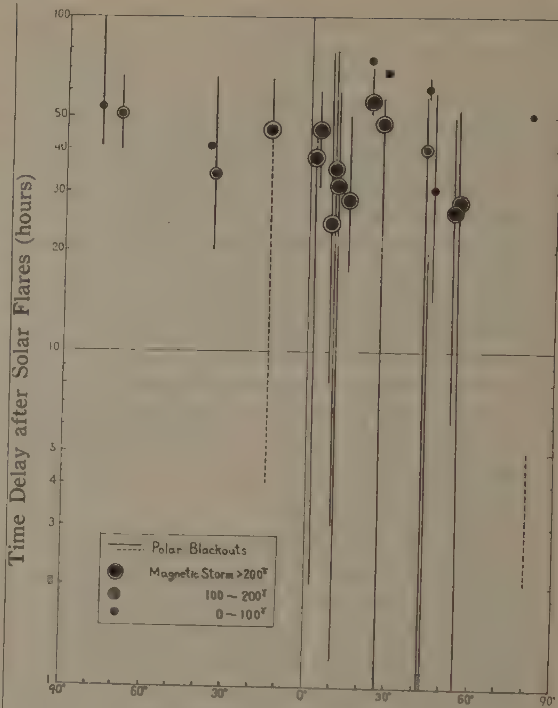

Fig. 1. Time Delays of Polar Blackouts and Magnetic Storms associated with Type IV Outbursts.

NISHIDA A. (Geophysical Institute, Tokyo University) **On the Earth Storm I. Stability of Solar Corpuscular Stream**——It has been strongly believed that the earth storm is caused by the arrival of corpuscular stream originating from the sun. But the physical state of the stream can hardly be determined from direct observation, and is estimated mostly from the interpretation of the observed disturbances on the earth. It would be clear anyway that the stream must be the one that is not only capable of explaining the terrestrial disturbances, but also able to travel stabely from the sun to the earth, i. e. without dissipating its energy density too much to give rise to the observed phenomena. From this standpoint, it is tried to see whether the non-magnetized stream can be the cause of the earth storm or not. The interplanetary space is assumed to be filled with plasma of density 10^3 cm^{-3} and of temperature 10^5 K. Of the interplanetary magnetic field, two cases are assumed. In the first it is assumed to be negligible and in the second, radial field of 10^{-4} Gauss is assumed to exist. The effect of collision between stream and interplanetary plasma is negligible on protons in the stream and on interplanetary plasma,

but it makes electrons in the stream retard from protons, and so the non-magnetized stream comes to be composed only of protons, thus giving rise to the electromagnetic field. But it can be shown that the space charge thus produced is sufficiently neutralized by the density change of electrons in the interplanetary space, and the stream can propagate stably, i.e. without changing much of its density and velocity. It can be concluded therefore that the non-magnetized stream, though it comes to be composed only of protons, is stable enough to be a cause of the earth storm.

MATSUURA N. (Geophysical Institute, Tokyo University) **On the Earth's Storm II. Interaction Between the Solar Corpuscular Stream and the Earth's Magnetic Field**——Effect of the stream of solar particles upon the exosphere was examined. Exosphere can be regarded as a good conductor even if considerable amount of atoms as estimated by Johnson exist. When solar stream compresses the earth's magnetic field in the initial phase, the exospheric gas may also be compressed. Heating of exospheric gas owing to the adiabatic material compression is not so important and it may not be a cause of main phase. In order to interprete the main phase of magnetic storm, the problem of random penetration of solar corpuscles under the influence of irregular magnetic field is dealt with. Solar particles of energy 20 KeV may penetrate into the exosphere near the five times of the earth's radius from the center of the earth about 10^5 seconds after the arrival of solar stream. Then, maximum density of the penetrated particles becomes nearly 10^3 cm^{-3}, when the stream density is assumed to be 10^3 cm^{-3}. The total energy of the penetrating particles can be estimated as the order of 10^{24} ergs. It seems that this value is sufficient for expansion or pulling away of magnetic field as much as causing the main phase of magnetic storm. A mechanism of particle acceleration by gyro-relaxation was discussed. However, the time necessary for acceleration up the auroral particle energy may become the order of 10^5 seconds, so this mechanism is not efficient to demonstrate the rapid change of forms of auroral display.

OGUTI T. (Geophysical Institute, Tokyo University) **On the Earth Storm III. Interrelations Among the Upper Atmosphere Disturbance Phenomena Over the Polar Region**——Inter-relations among the upper atmosphere disturbance phenomena in the auroral zone are discussed with the aid of observation at the Syowa Station (60°00′S in latitude and 39°35′E in longitude). Results obtained can be summarized as follows; 1. Geomagnetic bay type disturbances, ionospheric disturbances represented for example by anomalous increase in fEs and abrupt increase of auroral luminosity λ5577 in zenith begin simultaneously with each other within the accuracy of observation. It is noteworthy that the onset of increase of auroral zenith luminosity not of total activity is simultaneous with those of the other disturbance phenomena. 2. Ionospheric blackout follows geomagnetic disturbances and auroral displays in morning-daytime site of the auroral zone, while increase in fEs follows those in evening-night time site. 3. Amounts of physical quantities, i.e. decrease of geomagnetic horizontal intensity, increase in fEs and auroral λ5577 zenith intensity, are found to be consistent with each other, if it is postulated that these disturbance phenomena are due to anomalous ionization in the lower ionosphere with simultaneous excitation during auroral displays.

NAGATA T. and KOKUBUN S. (Geophysical Institute, Tokyo University) **On the Earth Storm IV. Geomagnetic Disturbances in the North and South Polar Regions**——It was pointed out by one of the writers that the variation of K-indices at Syowa base in Antarctic fairly coincides with that of Kp, and that K-indices at Syowa increase parallel to Kp after sudden commencement of magnetic storms except one case of 17 magnetic storms which occurred during five months from February to July in 1959, and some local disturbances were found, i.e. difference of K and Kp is 2 or 3. In order to examine geomagnetic correspondences of the north and south polar regions in more concrete forms, the photocopies of the ordinary magnetograms at four antarctic observatories and two arctic's during IGY were analysed. The average S_D-field in the south polar region was discussed from the statistical standpoint in the following form, S_D=$A(T_S)$ $S_D{}^\circ(t)$, where $S_D{}^\circ(t)$ is an idealized field pattern depending upon local time, and $A(T_S)$ is the amplitude of S_D varying its value with storm time. The distribution of the current arrow with respect to local time is nearly symmetric to the equatorial plane with the typical pattern of the S_D-variation in the north polar region, obtained by the analysis of the data during the Second Polar Year. One to one correspondence of

geomagnetic disturbances between the geomagnetic conjugate points; Little America in Antarctic and Baker Lake in Arctic, were examined. It was found that geomagnetic bays at the geomagnetic conjugate points in high latitude show high connection with each other, especially when both the stations at night side.

TOHMATSU T. (Geophysical Institute, Tokyo University) **On the Earth Storm V. Energy and Flux of the Corpuscular Streams Impinging the Earth's Upper Atmosphere**——Energy and flux of the energetic protons and electrons invading the polar upper atmosphere during the earth storm are estimated from several observational informations obtained by means of various optical and radio techniques, with the aid of available ionization and excitation cross sections. Studies have been made in concerning with the following three zones: (i) Polar cap: The anomalous ionization in the lower polar ionosphere which can be observed as the increase of f-min or radio black-out before the onset of the geomagnetic sudden commencement may be produced by the solar protons with incident energy 1~100MeV. The flux is estimated to be $10 \sim 10^3$ protons/cm^2-sec in order to cause the observed absorption of ordinary radio waves. No optical phenomena visible are expected in this region; (ii) Auroral zone: Both protons and electrons may contribute equally to the ionization and excitation in the auroral zone according to the stage of earth storm. The flux of protons with energy higher than 100 KeV may be of the order of 2×10^7 protons/cm^2–sec, when it is estimated from the intensities of hydrogen emissions in the homogeneous arc. As has been shown by the recent rocket observation of aurora producing particles, electrons can be the main agent for general luminosity and sporadic ionization in the aurora. A theoretical investigation of simultaneous optical excitation and ionization is made by considering an electron flux which is directionally isotropic at the top of the atmosphere and with the energy spectrum proportional to E^{-1} in the range from 1 KeV to 100 KeV, being consistent with the rocket results. The theoretical results are compared with the observed; (iii) Subauroral zone: The invisible aurora is likely to occur more frequently than it has been believed in the lower latitudes, forming an isolated fringe to the main luminosity in the north. The preferential enhancement of [OI] 6300 radiation may be caused by the dissociative recombination of ionized oxygen molecules with the electrons in the ionospheric F regions. Anomalous increase in the intensity could be explained by either (1) the ionization of the upper atmosphere above 150 km by the slow electrons with energy 10~100 eV or protons with energy 1~10 KeV or (2) the downward drift of the electron-ion swarm in the F region by the electric field produced locally during the earth storm.

KUBOKI T. and OHCHI K. (Magnetic Observatory, Kanoya) **On the Three-Hour-Range Indices K at Kanoya Observatory**——The authors determined K-index scale, similarly at Kakioka, Shimosato, and Aso; K=9 corresponds to 300 γ at Kanoya magnetic observatory, and they researched characteristics of K-indices in 1958. The results are shown as follows. (1) The diurnal variation, seasonal variation and frequency distribution of K-indices are almost the same as those of Kakioka respectively and they found hardly characteristics of equatorial type disturbance. (2) In comparison among Kakioka, Memambetsu and Kanoya for K-indices, it was very rear that the K differed by more than 2 in every interval and ΣK differed by more than 4. (3) Almost K are caused by the variation of horizontal intensity but from 6h to 9h (L.T.) in summer, the K-indices are affected by declination. This characteristics have been shown more distinctly than at Kakioka. (4) For the question of cause of K-indices, they consider as follows. Generally K less than 3 is caused by irregular variations (perhaps equatorial type disturbance), and K more than 4 is caused by bay type variations. K caused by magnetic storm disturbance shows values over than 6, but the percentage of this disturbance is very poor. Generally, as previously reported, cause of the K-indices is due to bay type variation and various variations of K-indices are almost the same as bay type variations. (5) In comparison among variations of K-indices at Honolulu, Huancayo and other 10 stations, they did not find out characteristics of equatorial type disturbance at Kanoya, geomagnetic latitude 22.5°N (geographic latitude 31.4°N). For this results they conclude, the dip shows large angle for geomagnetic latitude and this is a characteristic in the vicinity of Japan.

MAEDA K. (Kyoto University) **Image of a Magnet Caused by an Anisotropic Conductive Disc**——The initial phase of a magnetic storm is thought to be interpreted by a kind of mirror effect, which is caused by the conductive front of a charged particle stream

from the sun. A simple theory of this phenomenon was given already in "A Treatise on Electricity and Magnetism" by J.C. Maxwell. The present paper deals with a case, in which the conductivity of a front is anisotropic owing to the presence of magnetic field in the stream. As a model of this case it is assumed that an infinite disc with a finite depth consists of electrons, protons and neutral particles and contains a magnetic field parallel to the disc plane, and a magnet approaches to the disc with a constant velocity. An approximate treatment of the above problem is given. The result is as follows. (1) The image by the anisotropic conductive disc can be treated as consisting of two components, the behaviours of which are represented by different image strengths and life times. (2) The one component is controlled by the magnetic field involved in the disc, and the other is not affected by it. (3) The image as a whole is not parallel to the primary magnet and as a consequence a kind of distortion originates. (4) When the magnetic field involved in the disc is in disorder, the mirror becomes ineffective and decays rapidly, unless the magnetic field is weak. Some discussions are also given on the possible correlation to the phenomena of sudden commencement and initial phase of a magnetic storm and invasion of a magnetic cloud into the earth's atmosphere.

MAEDA H. and YAMAMOTO M. (Geophysical Institute, Kyoto University) **A Note on Daytime Enhancement of the Amplitude of Geomagnetic-Storm Sudden Commencements in the Equatorial Region**——By analysing 50 SC's during the IGY at eleven stations in the equatorial region, it is found that: (1) The daytime enhancement in amplitude of SC's occurs at stations less than 20° in geomagnetic dip, and abnormally large amplitudes appear at stations very close (within about 3° in dip) to the dip equator; (2) At stations higher than 20° in dip, no appreciable diurnal variation in SC's is seen; (3) The magnitude of SC's in the night-time is almost the same for all equatorial stations. These results may suggest that the sudden commencement of magnetic storms consists of two parts; one is of atmospheric origin and the other is of outer atmospheric origin. The former seems to be due to an electric current which probably flows in the Sq-current layer, and the latter seems to be caused in such a manner as Chapman-Ferraro model. And the separation of these two parts may be possible by using night-time values of SC's.

KUBOKI T. and OHCHI K. (Magnetic Observatory, Kanoya) **Some Characteristics at Kanoya Magnetic Observatory.**——The magnetic observation started on January, 1958 at Kanoya. The authors have researched some characteristics there and the results are shown as follows. (1) The solar diurnal variations are almost the same as Kakioka's, that is, the diurnal variation of vertical component shows large one unexpectedly, and the diurnal variation of Declination shows more excellence than Kakioka's. (2) Generally, the chance of occurrence of so-called E type diurnal variations occurs seldom, and they have found occurrence of it more in winter than summer. Using the vector diagrams at Memambetsu, Kakioka, Shimosato, Aso and Kanoya, they explained the change of diurnal variation and they often found change of diurnal variation which is caused by removement of over-head current system. (3) The values of $\Delta Z/\Delta H$ for variations of ssc, si, bay and storms show about 0.5; this is smaller than Kakioka's, but too much larger than expected value (0.3). (4) The lunar diurnal variations in earth-current are exceedingly great, but magnetic lunar diurnal variations are almost similar to those of Kakioka. The L variations of declination show the most distinct form, but the L variations of Horizontal and Vertical component are not so clear. The maximum range of lunar diurnal variation in each component is shown as follows. $D=6\sim7\gamma$. $H=3\sim5\gamma$. $Z=1\sim3\gamma$. As a whole, forms of the L variation in winter are more distinct than in other seasons, and the magnetic L variations at Kanoya are normally and almost same as those at Kakioka and Memambetsu. (5) In characteristic of earth-currents, the direction of vector for each variation shows different direction for its period respectively, especialy the direction of mean vector in the diurnal variation and the direction of short period variation meet at right angles and the direction of mean vector in diurnal variation runs parallel to the coast line. And then the pc type variation excels in NS component in opposit to other variations. (6) They have examined the difference of earth-current potentials to investigate abnormal variation accompanied with other geophysical phenomena, but as a result, they did not find abnormal variation on the difference of earth-current potentials for earth-quake on Mar. 4th, 1960 at the district of Yaku Island (Seismic intensity 4).

昭和35年 9 月25日 印刷
昭和35年 9 月30日 發行
第12巻 第1號

編輯兼發行者 日本地球電氣磁氣學會
代表者 長 谷 川 万 吉

印刷者 京都市南區上鳥羽唐戸町63
田 中 幾 治 郎

賣捌所 丸 善 株 式 会 社 京 都 支 店
丸善株式會社 東京・大阪・名古屋・仙台・福岡

JOURNAL OF GEOMAGNETISM AND GEOELECTRICITY

Vol. XII No. 1

1960

CONTENTS